Critical Reviews in Solid State and Materials Sciences, 27(2):73–117 (2002)

Copper Indium Selenides and Related Materials for Photovoltaic Devices

Billy J. Stanbery
HelioVolt Corporation, 1101 S. Capital of Texas Highway, Suite 100F, Austin, TX 78746-6490

ABSTRACT: Solar cells based on copper ternary chalcogenide compounds and alloys have emerged over the last 20 years as a promising solution to the problem of high-cost solar cells. Solar power conversion efficiencies exceed 21% in laboratory devices using thin films of these materials,[1] and their characteristic thinness results in negligible direct materials costs per unit area compared with wafers.[2] Photovoltaic devices made from these materials have also been shown to be intrinsically stable,[3] circumventing the historical disadvantage of degradation typical of earlier thin film solar cell technologies. However, these copper chalcogenide devices and materials are relatively complex. This article provides an overview of the current state of our scientific understanding and technological development of them.

TABLE OF CONTENTS

I. Introduction 74
II. Physical Properties of Cu–III–VI Materials 75
  A. Phase Chemistry of Cu–III–VI Material Systems 75
    1. The Cu–In–Se (CIS) Material System 75
    2. The Cu–Ga–Se (CGS) Material System 77
    3. The Cu–In–S (CISu) Material System 78
  B. Crystallographic Structure of the Ternary CIS Compounds 78
    1. α–CIS (Chalcopyrite $CuInSe_2$) 78
    2. δ–CIS (Sphalerite) 80
    3. β–CIS ($Cu_2In_4Se_7$ and $CuIn_3Se_5$) 80
    4. γ–CIS ($CuIn_5Se_8$) 81
    5. Metastable Crystallographic Structures — CuAu Ordering 81
    6. Defect Structure of the α–CIS Lattice 82
  C. Optical Properties of Ternary Cu–III–VI Compounds 86
    1. Variation of Optical Absorption with Composition. 86
    2. Lattice Dynamics and Infrared Optical Properties 87
    3. Optical Properties of α–CIS and β–CIS 87
    4. Optical Properties of α–CGS 88
    5. Optical Properties of α–CISu 89
  D. Alloys and Dopants Employed in CIS Photovoltaic Devices 89
    1. Gallium Pseudobinary Alloy — CIGS 89
    2. Bandgap Dependence on CIGS Composition 90
    3. Sulfur Pseudobinary Alloy —CISS 91
    4. Alkali Impurities in CIS and Related Materials 91
  E. Electronic and Ionic Transport in CIS Photovoltaic Device Materials 93
    1. Electronic Carrier Concentration and Composition 93
    2. Electronic Transport in CIS 94
    3. Electromigration of Copper in CIS 96

1040-8436/02/$.50
© 2002 by CRC Press, Inc.

III. CIS Photovoltaic Devices 96
A. CIS Photovoltaic Device Structures 97
1. Absorber Structures 98
2. Emitter Structures 100
3. Ohmic Contacts 101
4. Superstrate Devices 102
B. Fabrication Methods for CIS Absorber Films 102
1. Codeposition 102
2. Metal Chalcogenization 103
3. Post-Deposition Thermal Processing 104
C. Opto-electronic Properties of CIS Devices 104
1. Phenomenological Characteristics 104
2. Theory of Operation 105
IV. Summary: Future Prospects for CIS Photovoltaics 106
References 107

I. INTRODUCTION

Any review of the prior research in this long-studied field must first cite a number of the excellent reviews already published in the literature. Nevertheless, the field is rapidly progressing, and this critical review strives to highlight from this author's perspective both some of those research results that have been reviewed previously and those too recent to have been available to prior authors. The earliest comprehensive review of chalcopyrite semiconducting materials[4] by Shay and Wernick is a classic reference in this field. It focused primarily on the physical and opto-electronic properties of the general class of I–III–VI_2 and II–IV–V_2 compound semiconductors. More recent reviews specifically oriented toward copper indium selenide (CIS) materials and device properties[5-10] are also recommended reading for those seeking to familiarize themselves with key research results in this field.

There are also a number of excellent books and reviews on photovoltaic device physics,[11-13] on the general subject of solar cells and their applications,[14,15] and others specifically oriented towards thin-film solar cells,[16,17] the class to which CIS solar cells belong. Finally, a nontechnical but concise and current overview of solar cell technology was published recently by Benner and Kazmerski.[18]

The first solid-state photovoltaic (PV) device was demonstrated in 1877 and consisted of a rod of selenium held between two wire electrodes.[19] The addition of copper and indium and creation of the first CIS PV device occurred almost 100 years later in 1973,[20] when a research team at Salford University annealed a single-crystal of the ternary compound semiconductor $CuInSe_2$ in indium. Almost all subsequent Cu–In–Se thin-film deposition process development for PV device applications have sought to make the compound $CuInSe_2$ or alloys thereof, but, in fact, generally result in a multiphase mixture,[21] incorporating small amounts of other phases. Researchers have not always been careful to reserve the use of the compound designation $CuInSe_2$ for single-phase material of the designated stoichiometry, an imprecision that is understandable in view of the difficulty of experimentally discriminating $CuInSe_2$ from some other compounds in this material system, as well as this phase's inherent stoichiometric variability. The compound designations such as copper indium diselenide ($CuInSe_2$) are reserved herein for reference to single-phase material of finite solid solution extent, and multiphase or materials of indeterminate structure composed of copper, indium, and selenium are referred to by the customary acronym, in this case CIS.

II. PHYSICAL PROPERTIES OF CU–III–VI MATERIALS

This section provides a detailed discussion of the physical properties of the principal copper ternary chalcogenides utilized for PV devices, including their thermochemistry, crystallography, and opto-electronic properties. All state-of-the-art devices rely on alloys of these ternary compounds and employ alkali impurities, so the physical properties and effects of these additives will be presented, with an emphasis on their relevance to electronic carrier transport properties. This foundation provides a basis from which to address the additional complexities and variability resulting from the plethora of materials processing methods and device structures that have been employed successfully to fabricate PV devices utilizing absorbers belonging to this class of materials. Those device structures, and their processing methods and opto-electronic characteristics, are described subsequently, in Section III.

A. Phase Chemistry of Cu–III–VI Material Systems

Significant technological applications exist for Ag–III–VI_2 compounds as nonlinear optical materials,[22] but almost all PV devices being developed for solar energy conversion that utilize ternary chalcogenides are based on the Cu–III–VI material system. Although initially the reasons for this may have been historical, this review demonstrates that fundamental physical properties of these materials render them uniquely well suited, and underlie the research community's continuing development of them, for PV applications.

1. The Cu–In–Se (CIS) Material System

The thermochemistry of the Cu–In–Se ternary material system has been studied intensely, but significant inconsistencies abound and the incompleteness of the extant scientific literature will become apparent to the reader. One superficial inconsistency is in the Greek letter designations employed to describe the various phases, but even today there persist more substantive disagreements, for example, on the number of phases found in the ternary phase field. To avoid confusion all discussions herein that employ Greek letter designations to identify thermodynamic of phases will use the identifiers from the work Boehnke and Kühn.[23]

Experimental studies that require bulk synthesis are extraordinarily difficult because of the high vapor pressure of selenium and reactivity of copper with quartz ampoules typically used.[24] Therefore, it is difficult to ensure that the thermodynamic system remains closed during synthesis and that the resulting constitution accurately reflects the starting material ratios. Thus, it is difficult to judge whether syntheses intended to lie on the Cu_2Se – In_2Se_3 pseudobinary section remain so, hence whether that section is actually an equilibrium tie-line. Although considerable progress has been made in the bulk synthesis of these compounds,[9] uncertainties such as these persist to this day in efforts to assess the phase diagram.

The earliest published study of the Cu–In–Se phase[25] was restricted to a segment of the presumably pseudobinary section between the compounds Cu_2Se and In_2Se_3, and centered on the equimolar composition corresponding to $CuInSe_2$. Several key features of Palatnik and Rogacheva's results have been confirmed in subsequent studies of this system, albeit with different values of the critical point temperature and compositions. First, congruent melting of the solid compound with a composition near that of $CuInSe_2$ at a temperature somewhat less than 1000°C (986°C) is observed. Second, a congruent first-order solid-solid (α to δ) phase transition at a lower temperature (810°C) of that high-temperature phase *via* a crystallographic order-disorder transition between the cation-disordered sphalerite structure (δ phase) and the chalcopyrite structure (α phase) is observed. Third, temperature-dependent extensions of the phase homogeneity range of the chalcopyrite structure to somewhat indium-rich compositions, but none toward copper-enrichment are observed. Fourth, peritectoid decomposition of the sphalerite phase at its lowest stable temperature into the chalcopyrite and a relatively indium-rich defect-tetragonal structure is observed.

Extension of the characterization of the Cu–In–Se ternary phase field to compositions off the Cu_2Se–In_2Se_3 section was finally published in the 1980s by three groups,[23,26,27] although there are significant discrepancies among them. Boehnke and Kühn find four phases on the indium-rich side of the pseudobinary section between the compositions of $CuInSe_2$ and In_2Se_3, whereas Fearheiley and co-workers report seven phases based primarily on crystallographic studies by Folmer et al. [28] Bachmann[29] and Palatnik[25] both found a congruently melting copper-rich compound on this section with a composition Cu_5InSe_4 (analogous to the mineral bornite, Cu_5FeS_4), reported to be unstable at room temperature. Although this compound was not found in subsequent studies, the copper-rich compound $Cu_{13}In_3Se_{11}$ later reported by Bachmann[30] has been confirmed recently.[31] Bachmann and co-workers found two critical point compositions for congruent melting of the solid phases on the indium-rich side of this section: at 55% In_2Se_3 mole fraction (corresponding to about 22 at.% copper) and at 75% In_2Se_3 mole fraction (corresponding to the compound $CuIn_3Se_5$), whereas the others find only one. A more recent study suggests that there is only one congruently melting composition on this segment of the liquidus at 52.5 mole% In_2Se_3.[32] These and other studies have been assessed by Chang and co-workers[33] resulting in the T–X section of the phase diagram (temperature-dependence of the phase constitution along a line segment within the ternary composition triangle) shown in Figure 1, which is referenced in further discussions throughout this article.

Another important study has been conducted more recently that focused on a relatively restricted composition and temperature range directly relevant to typical CIS photovoltaic device materials and processing.[34] Its most important conclusions were that the composition of the α–δ congruent phase transition occurs at 24.5 at.% Cu (50.8 mol% In_2Se_3) rather than the stoichiometric composition of $CuInSe_2$, and that the Cu_2Se – $CuInSe_2$ phase boundary at room temperature corresponds to this same composition. Their data also confirm the retrograde phase boundary between the α–phase and β–phase at temperatures below the α+β–>δ eutectoid transition temperature (which they find to be 550°C, near Rogacheva's but much lower than Boehnke's and Fearheiley's results), with this boundary at room temperature at 24.0 at.% Cu (51.6 mol% In_2Se_3).

Very recently a series of three articles have been published that extended the preliminary study just cited to the entire ternary Cu–In–Se phase field.[31,35,36] This undoubtedly constitutes the most comprehensive study of phase equilibria in this system to date. Those studies concluded that there are four different primary manifolds of crystallization of the α-CIS phase and that thin films of CIS typically exhibit a nonequilibrium phase structure corresponding to a quenched high-temperature equilibrium structure. Their studies of supercooled (metastable) bulk samples along the α-CIS/$Cu_{2-\delta}Se$ quasibinary section showed that quenching can result in copper supersaturation, but that in equilibrium the stoichiometric composition $CuInSe_2$ is a two-phase mixture of copper-deficient α-CIS and $Cu_{2-\delta}Se$.

Recently, this author developed the first computational free energy defect model for $CuInSe_2$ that includes the effects of defect associates (complexes).[37] Statistical mechanical entropy calculations were combined with published phase diagrams and *ab-initio* quantum mechanical calculations of defect formation enthalpies from the literature. A novel method was developed to solve this problem, combining a lattice cluster expansion with the stoichiometric reaction analysis approach. This model correctly predicts the α/β ternary phase boundary and predicts the existence of significant kinetic barriers to thermal equilibration of nonstoichiometric CIS at temperatures below the peritectoid phase transformation in the Cu–Se system near 123°C. The latter prediction is consistent with the report by Gödecke and co-workers of a wide composition range of metastable single-phase α-CIS produced by supercooling.[31]

Perhaps the most significant result of this author's thermodynamic phase-diagram modeling to date is the prediction that at temperatures below 400°C the lowest possible free energy for single-phase α-CIS with its maximum equilibrium copper content is off the pseudobinary section, when the lattice is enriched with an excess of

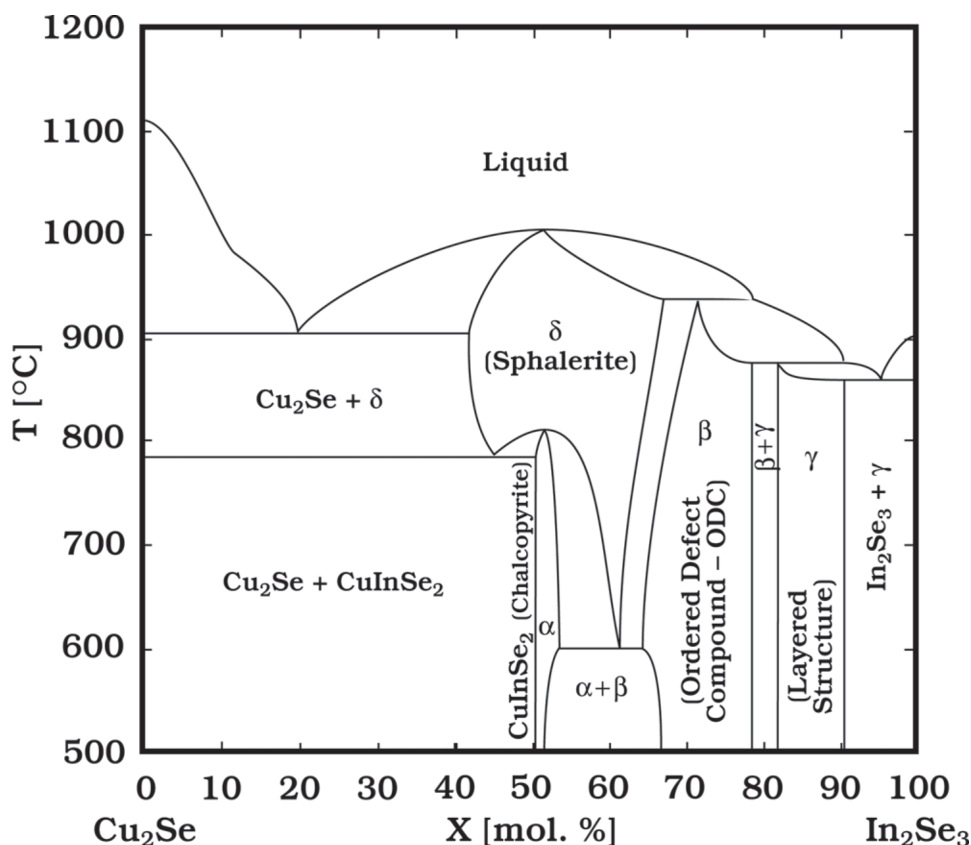

FIGURE 1. Adapted from a published assessment of the phase diagram along the Cu_2Se – In_2Se_3 pseudobinary section of the Cu–In–Se chemical system.[33]

0.1 to 0.2% selenium. This small deviation off the pseudobinary section has not been reported experimentally, perhaps because its magnitude is very nearly the absolute calibration and resolution limit of current chemical analysis methods for the principal constituents of nonstoichiometric multinary solids.

2. The Cu–Ga–Se (CGS) Material System

The phase diagram of the Cu–Ga–Se ternary material system remains less well characterized and even more controversial than that of Cu–In–Se.[38] The earliest detailed phase equilibrium study,[39] once again restricted to the presumably pseudobinary Cu_2Se – Ga_2Se_3 section within the ternary phase field, reported the existence of one high-temperature disordered phase and four room temperature stable phases. Two of those latter phases were solid solutions based on the terminal binary compounds, one was a phase (β) with the $CuGaSe_2$ composition as its copper-rich boundary, and the last was a relatively indium-rich phase (δ) with a layered structure. The only other comprehensive study of this ternary phase field[40] failed to confirm the existence of that δ phase or the associated compound $CuGa_5Se_8$.

Both studies, however, found that the stoichiometric compound $CuGaSe_2$ has a chalcopyrite structure and does not melt congruently, but instead undergoes peritectic decomposition at a temperature of 1050 to 1030°C. The earlier study by Palatnik and Belova[39] characterized the resulting gallium-rich solid, representing the copper-rich boundary of the high-temperature (γ) phase, as the compound $Cu_9Ga_{11}Se_{21}$ (55 mol% Ga_2Se_3) possessing a disordered sphalerite crystal structure. They found the associated liquid composition at the peritectic to be 38 mol% Ga_2Se_3.

A more recent study of $CuGaSe_2$ crystal growth by the gradient freeze technique[38] provides evidence contradictory to the earlier reports

that the compound decomposes peritectically and suggests instead that it decomposes congruently and that the earlier studies mistook a solid-phase transformation that they find at 1045°C for peritectic decomposition. Resolution of these discrepancies requires further scientific inquiry, and a comprehensive assessment is needed.

Perhaps most importantly for photovoltaic-related process development is the consensus between both of these studies of the phase diagram that the homogeneity range of the chalcopyrite phase extends significantly to gallium-rich compositions along this section, as it does in $CuInSe_2$, but not measurably toward compositions more copper rich than that of stoichiometric $CuGaSe_2$.

3. The Cu–In–S (CISU) Material System

Unlike the other two ternary copper chalcopyrites discussed herein, $CuInS_2$ occurs naturally, as the mineral roquesite. The earliest comprehensive study of the Cu_2S – In_2S_3 section was conducted by Binsma and co-workers.[41] They found four room-temperature phases, two corresponding to the terminal binaries and two others containing the compounds $CuInS_2$ (γ) and $CuIn_5S_8$ (ε). They did not report the low-temperature homogeneity range of these phases other than to note that for $CuInS_2$ it was below their detection limits. An earlier study, however, reported the homogeneity range of γ–$CuInS_2$ to be 50 to 52 mol% In_2S_3 and that of ε–$CuIn_5S_8$ from the stoichometric composition to almost 100% In_2S_3.[42] At higher temperature, but below the chalcopyrite to sphalerite congruent solid phase order–disorder transition temperature at 980°C, Binsma found that the homogeneity range of γ–$CuInS_2$ extended to copper-rich compositions, unlike the ternary phases containing $CuInSe_2$ and $CuGaSe_2$. A third solid-phase transition of the sphalerite structure was detected at 1045°C, just below the congruent melting temperature of 1090°C.

Much of the thermochemical data published on the Cu–In–S ternary system prior to 1993 have been incorporated into an assessment published by Migge and Grzanna.[43] A more recent experimental study of the $CuInS_2$ – In_2S_3 subsection of the ternary phase field[44] found similar solid phase structures and transition temperature as those reported by Binsma, including the congruent melting of the indium-rich phase with a spinel structure and compositions around that of the compound $CuIn_5S_8$. They also found, however, an intermediate phase with a fairly narrow homogeneity range around the 62.5 mol% In_2S_3 composition of the compound $Cu_3In_5S_9$, which was reported to exhibit a monoclinic structure.

Another recent study extended the Cu–In–S ternary phase field characterization to the CuS–InS join,[45] and confirmed that the Cu_2S–In_2S_3 pseudobinary section appears to be an equilibrium tie-line in this ternary phase field. They find that the room temperature homogeneity domain for the roquesite γ–$CuInS_2$ phase is limited to 52 mol% In_2S_3 but extends toward CuS enrichment as much as 6 mol%. They also find that the two indium-rich ternary phases on the pseudobinary section described in the previous paragraph do not extend to this join.

B. Crystallographic Structure of the Ternary CIS Compounds

This section is limited to a discussion of those compounds that are stable at room temperature, with the exception of δ–CIS. This is not a particularly serious restriction for subsequent discussions of thin film growth techniques, because all of those under development for device applications take place at temperature well below the solid-phase transition and decomposition temperature of all of these compounds, with the possible exception of the β to δ-CIS transition, as discussed in the preceding section.

1. α–CIS (Chalcopyrite $CuInSe_2$)

The crystal structure of α–CIS is well established to be chalcopyrite, corresponding to the space group $I\bar{4}2d$. It is an adamantine structure, as are δ-CIS and β-CIS, characterized by tetrahedral coordination of every lattice site to its nearest neighbors. It is distinguished from the zincblende structure of the binary Grimm-Sommerfeld

compounds[46] by ordering of its *fcc* cation sublattice into two distinct sites, one occupied in the ideal structure by copper and the other by indium (Figure 2 (a)), and valency considerations require exactly equal numbers of each. Single-phase homogeneous crystals will for entropic reasons always exhibit some degree of disorder at room temperature irrespective of the deviation of their composition from the stoichiometric compound $CuInSe_2$, although such deviations will always increase that disorder. The chalcogenide atoms are located on another *fcc* lattice referred to as the anion sublattice. The two sublattices interpenetrate such that the four nearest neighboring sites to each cation site lie on the anion sublattice (Figure 2(b)) and conversely the four nearest neighboring sites to each anion site lie on the cation sublattice (Figure 2(c)). Each anion is surrounded by two Cu and two In site types, normally occupied by their respective atoms.

The very different chemical nature of the copper and indium atoms result in bonds between each of them and their neighboring selenium atoms with very different ionic character and lengths.[47] This bond-length alternation has the electronic effect of reducing the bandgap energy of the compound with the chalcopyrite structure, relative to that of the sphalerite structure with identical chemical composition, because the latter has a disordered cation sublattice. This bandgap reduction effect is known as optical bowing.

Bond-length alternation also has the effect of making the lattice constants of the chalcopyrite structure anisotropic in most cases. Binary compounds with the zincblende structure and the elemental compounds with a diamond structure require only one lattice constant to quantitatively characterize the crystal dimensions. The conventional unit cell of the chalcopyrite structure as shown in Figure 2 is equivalent to two cubic zincblende unit cells with sides of length a stacked in the c-direction and either compressed or dilated along that axis by a factor $\eta \equiv c/2a$, known as the tetragonal distortion.

The lattice constants of $CuInSe_2$ have been studied widely, but the early results by Spiess and co-workers[48] are in excellent agreement with the most recent measurements of bond lengths by

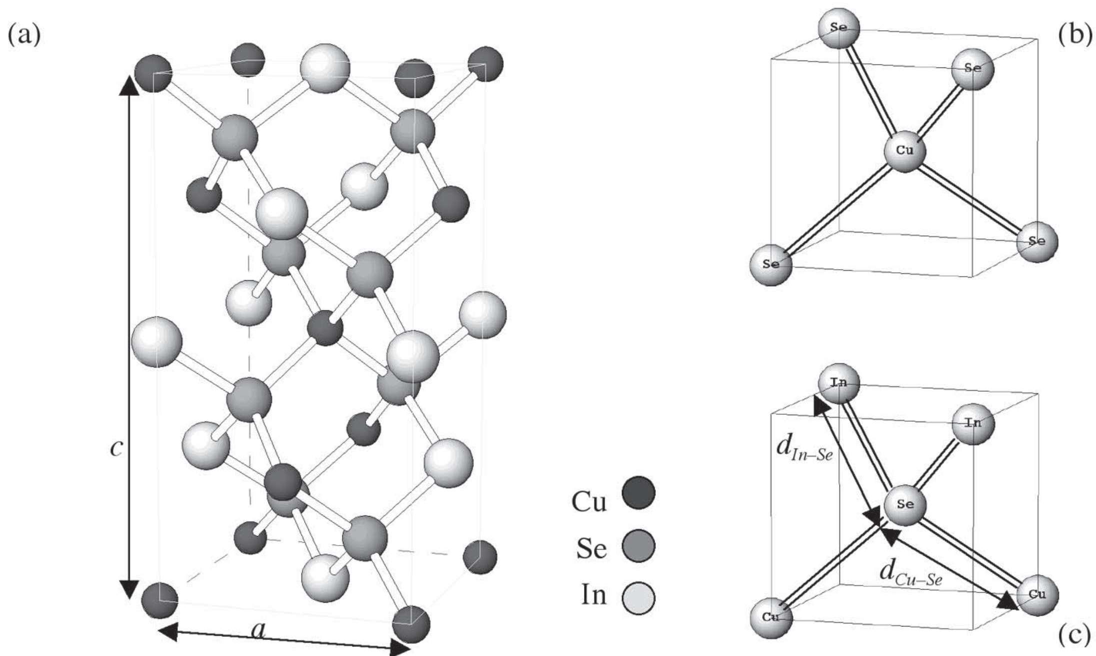

FIGURE 2. Schematic representation of $CuInSe_2$ chalcopyrite crystal structure: (a) conventional unit cell of height *c*, with a square base of width *a*; (b) cation-centered first coordination shell; (c) anion-centered first coordination shell showing bond lengths d_{Cu-Se} and d_{In-Se}.

EXAFS.[49] Those values are $a = 5.784$ Å, $c = 11.616$ Å (and hence $\eta = 1.004$), $d_{Cu-Se} = 2.484$ Å, and $d_{In-Se} = 2.586$ Å. A more comprehensive compilation of the various reports of lattice constant measurements for $CuInSe_2$ may be found in Chang's dissertation.[50]

2. δ–CIS (Sphalerite)

The δ–CIS phase is unstable at room temperature, and there is wide agreement that it forms from either solidification over a wide composition range of the ternary liquid or a first-order solid-phase transformation from either the α– or β–CIS phases or mixtures thereof (see Figure 1). The δ–CIS single-phase domain exhibits a congruent melting composition, for which the values of 1005°C at 52.5 mol% In_2Se_3[32] are accepted here. At lower temperature the domain of δ–CIS is limited by the eutectoid at 600°C,[34] where it decomposes into a mixture of α– and β–CIS. There remains inconsistency between the various studies over the compositional range of single-phase stability in the relevant high-temperature regime. Fearheiley's phase diagram[27] posits that this phase is limited on the copper-rich side by a eutectic associated with the putative compound Cu_5InSe_4, and stable to much higher In_2Se_3 mole fractions than found by Boehnke and Kühn,[23] or than shown in Figure 1.

The congruent first-order α–δ solid phase transition at 24.5 at.% Cu (50.8 mol% In_2Se_3) and 809°C[34] corresponds to the crystallographic order/disorder transformation from the chalcopyrite to sphalerite structure. The sphalerite structure is based on the zincblende unit cell (and hence does not exhibit tetragonal distortion), with no long-range ordering of copper and indium atoms on the cation sublattice. The persistence of short-range ordering in δ–CIS, specifically the dominance of 2 In + 2 Cu tetrahedral clusters around Se anions as found in α–CIS, has been predicted theoretically.[51]

3. β–CIS ($Cu_2In_4Se_7$ and $CuIn_3Se_5$)

It is doubtful that there is any part of the ternary Cu–In–Se phase diagram that is more controversial and simultaneously more important to understanding the operation of CIS PV devices than the indium-rich segment of the pseudobinary section containing the β–CIS phase domain shown in Figure 1. There is no agreement between the many studies of these relatively indium-rich materials on the phase boundaries' compositions, the number of different phases that lie between $CuInSe_2$ (α phase) and $CuIn_5Se_8$ (γ phase), or their crystallographic structure(s).

The situation in this field is very similar to that found in the study of the metal oxides, wherein there is considerable controversy as to whether nonstoichiometric phases are single phases with broad ranges of compositional stability, or a closely spaced series of ordered phases with relatively narrow ranges of stability.[52,§15.2-15.3]

The existence of the peritectoid decomposition reaction of δ–CIS to the α phase and another In_2Se_3-rich solid phase requires that between the compositions of $CuInSe_2$ and In_2Se_3 there lies at least one other distinct phase on their tie-line to satisfy the Gibbs phase rule. A review by Chang[53] finds at least eight different compounds ($Cu_2In_4Se_7$, $Cu_1In_3Se_5$, $CuIn_5Se_8$, $Cu_8In_{18}Se_{32}$, $Cu_7In_9Se_{32}$, $Cu_{14}In_{16.7}Se_{32}$, $Cu_2In_3Se_5$, $Cu_3In_5Se_9$), and structures based on eight different space symmetry groups ($I\bar{4}$, $I\bar{4}2m$, $P23$, $Pm3$, $P432$, $P\bar{4}3m$, $Pm3m$, $P\bar{4}2c$) have been proposed for β–CIS (although not all these compounds lie on the pseudobinary). Most of these proposed structures are members of the group of adamantine superstructures derived from the cubic diamond lattice structure.[54] Recently, a twinned structure that does not correspond to any of the 230 regular space groups[55,56] was also proposed for β–CIS.

Various nomenclatures are used by different researchers to describe the β–CIS compounds. They are sometimes referred to as P-chalcopyrite, a term created by Hönle and co-workers when they concluded that the structure possesses $P\bar{4}2c$ symmetry.[57] These structures are also sometimes referred to generically as "Ordered Defect Compounds" (ODC's), but it is important to understand that "ordering" in the context of this terminology refers to the regular arrangement of preferred crystallographic sites on which defects are found, which alters the symmetry properties of the lat-

tice. The defect distributions on those preferred sites in equilibrium might not have any long-range spatial order, although their statistical occupation probabilities nevertheless could be well defined.

It is beyond the scope of this review to attempt any resolution of this continuing controversy. Yet, numerous studies of polycrystalline CIS,[58] CISU,[59] and CIGS[60] PV absorber films have shown that the composition at the surfaces of those films that ultimately yield high-efficiency devices exhibits a [I]/[III] ratio of about $^1/_3$, corresponding to the compound $CuIn_3Se_5$ (except for nearly pure CGS where the ratio rises to about $^5/_6$ [60]). Resolution of these crystallographic and phase boundary uncertainties is essential to testing a recent theory that this behavior results from copper electromigration limited by the occurrence of a structural transformation at those compositions.[61] The existence of such a transformation is consistent with Fearheiley's evidence (which has not been confirmed) that the compound $CuIn_3Se_5$ melts congruently[27] and the crystallographic studies by Folmer[28] that find additional reflections in XRD spectra for pseudobinary compositions of 77 mol% In_2Se_3 or greater. The results of a recent EXAFS study directly prove that the crystallographic structure of $CuIn_3Se_5$ (75 mol% In_2Se_3) is defect tetragonal, containing a high concentration of cation site vacancies.[53]

4. γ–CIS ($CuIn_5Se_8$)

Folmer has pointed out[28] that the one common denominator between all of the structures found along the pseudobinary $Cu_2Se–In_2Se_3$ section is the persistence of a close packed lattice of selenium atoms. It is well known that different stacking sequences of such planes yields different crystallographic structures, for example, the hexagonal close-packed (…ABAB…) and the face-centered cubic (…ABCABC…), and that there are an infinite number of possible stacking arrangements.[62,§ 4] In cubic notation, these close-packed planes of the *fcc* structure are the {111} family (corresponding to the {221} planes of the chalcopyrite structure because of the latter's doubled periodicity along the *c*-axis).

Although the terminal indium binary compound In_2Se_3 on the pseudobinary section has been reported to possess several polymorphic structures, the low-temperature phases are characterized by hexagonal stacking of the close-packed planes of selenium atoms on the anion sublattice.[63] Hence, the existence of a structural transformation between the cubic stacking arrangement of the *fcc* anion sublattice of the chalcopyrite α–CIS structure, and the hexagonal stacking of In_2Se_3 at some point along that segment of this section is reasonable. The crystallographic studies by Folmer[28] described previously find additional reflections in XRD spectra that they index as (114) and (118), which represents evidence of at least partial hexagonal stacking of the close-packed layers of selenium anions, yielding a layered structure, presumably containing a high density of cation vacancies and antisites.

The segment on the $Cu_2Se–In_2Se_3$ section containing ≥ 77 mol% In_2Se_3 is assigned in Figure 1 to a single γ–CIS phase and a two-phase mixture of γ-CIS + In_2Se_3. Folmer concluded that there are three phases (excluding the terminal In_2Se_3) instead of one. Given the diversity of wurtzite-derived ternary defect adamantine structures with a hexagonal diamond structure,[54] the crystallographic data do not provide clear evidence in favor of either a few distinct phases in a closely spaced series or a pseudo-monophasic bivariant system[64] characterized by coherent intergrowth of two phases. Experimental evidence of coherent intergrowth on the copper-rich side of the $Cu_2Se–In_2Se_3$ section is discussed in the next section.

5. Metastable Crystallographic Structures — CuAu Ordering

Inasmuch as the chalcopyrite structure of α–CIS is itself an ordered variant of the sphalerite structure of δ–CIS, the issue of alternative ordering in the CIS material system has long been an active area of study. Vacancy ordering in conjunction with the indium-rich β–CIS phase has been described in an earlier section, but here alternative ordering of materials with a composition within the equilibrium stability range of α–CIS is discussed.

As early as 1992 a theoretical study by Wei and co-workers[51] of the α/δ–CIS order-disorder transition calculated that the energy of formation of the CuAu (CA) crystallographic structure (Figure 3) differed by only 0.2 meV/atom from that of the chalcopyrite (CH) at T = 0. In 1994 Bode,[65] however, reported evidence of CuPt–ordering (CP) from TEM studies of copper-rich CIS films. CuPt–ordering of III–V alloys has been observed widely since it was first reported in the AlGaAs system.[66] In CIS the calculated formation energy difference between the CP and CH structures (at zero Kelvin) was more than 25 times greater than the difference between that of CA and CH–ordered crystals.[51]

The equilibrium CH–CIS crystallographic structure shown in Figure 3(a) consists (in cubic notation) of alternating (201) planes of Cu and In atoms on the cation sublattice. The CA–CIS structure shown in Figure 3(b) consists of alternating (100) planes and CP–CIS structure consists of alternating (111) planes.[67] Consequently, each selenium atom in both the CH and CA structures is surrounded by two copper and two indium atoms in its first coordination shell, whereas in the CP structure each selenium is surrounded by either (3 Cu + In) or (3 In + Cu). This variation in local atomic structure is the fundamental reason for the similar formation energies of the CH and CA structures and their mutual disparity from that of the CP structure.

The apparent doubling of the periodicity along {111} (cubic notation) planes that was observed in the study that reported CP–CIS[65] was found in polycrystalline samples made by codeposition of Cu, In, and Se with an overall composition in the mixed β-$Cu_{2-\delta}Se$ + α-$CuInSe_2$ phase domain of the equilibrium phase diagram (Figure 1). Their interpretation has been challenged recently[68] based on the results of a careful study of CIS grown epitaxially on GaAs with a similar copper-rich composition, where it is shown that coherent intergrowth of a β–$Cu_{2-\delta}Se$ secondary phase can create an apparent doubling of lattice periodicity and thence of CuPt–ordering in copper-rich CIS. Coherent intergrowth of β–$Cu_{2-\delta}Se$ and $CuInSe_2$ has been suggested by other researchers to be an energetically favorable strain relief mechanism[69] because these two compounds share isomorphic, nearly identical Se sublattices.

CuAu–ordering (CA) of the Cu–III–VI_2 compounds was first detected experimentally by TEM in $CuInS_2$[67] indium-rich MBE–grown epilayers where the formation of a secondary $Cu_{2-\delta}S$ phase is unlikely. Recently, CA ordering has been demonstrated in $CuInSe_2$ in both copper- and indium–rich materials grown by Migration-Enhanced Epitaxy (MEE)[70] using XRD, TEM, and Raman scattering detection techniques.[71,72] Further studies of the electronic and optical properties of CA–CIS are needed to assess their impact on PV device absorber materials, which are very likely to often incorporate nanoscale domains of this crystallographic polytype.[72]

6. Defect Structure of the α–CIS Lattice

The study of the defect structure of α–CIS has probably generated more of the literature on α–CIS than any other fundamental scientific issue. Pure α–CIS is amphoteric: its conductivity type and carrier density varies with composition. It is incorrect to say, however, that these electronic transport properties in real materials are determined by composition alone, because the defect structures that must be controlling them are empirically found to vary dramatically between compositionally indistinguishable materials.

Conceptually, the densities of defect structures found in a single-phase material system in equilibrium must be determined uniquely by the composition, temperature, and pressure, or else the Gibbs potential, a function of these variables, is not a legitimate state function for the system. The only intellectually satisfactory resolution of this conundrum is to conclude that complete thermodynamic equilibrium is not often found in real CIS materials. As described in the previous section, recent calculations and experimental results confirm[71,73] that the free energy associated with the formation of some defect structures is so small that little increase in thermodynamic potential results, and hence there is insufficient driving force to ensure their elimination under many synthesis conditions. Furthermore, formation of many atomic defects requires bond breaking and atom transport processes. At low deposition or synthesis temperature it is expected that these kinetic

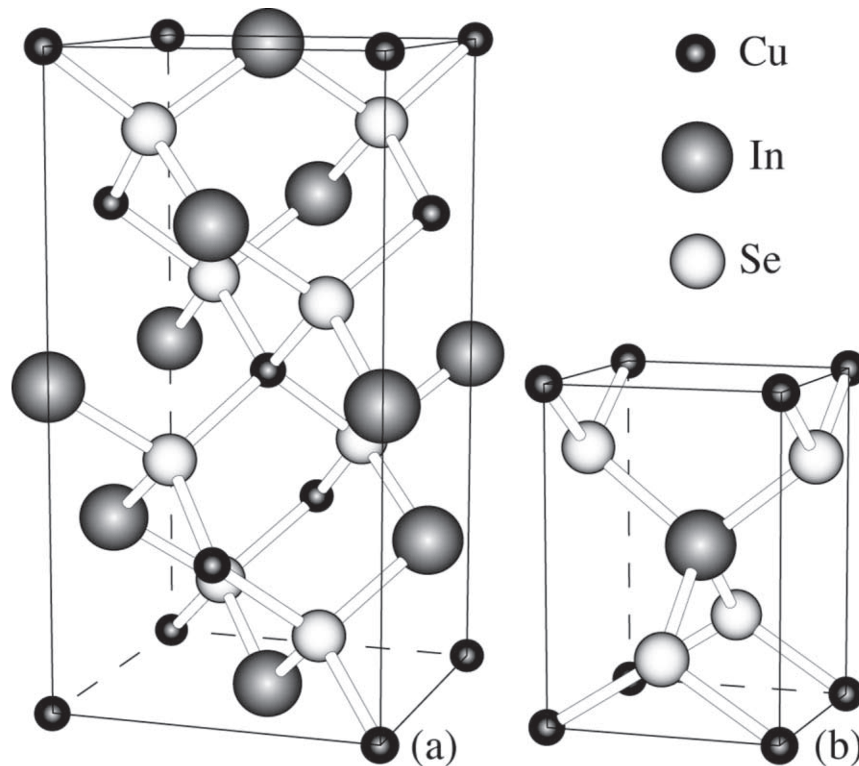

FIGURE 3. Comparison of the crystallographic unit cells of $CuInSe_2$ polytypes: (a) chalcopyrite (CH) structure, and (b) CuAu (CA) structure.

processes will limit the approach to equilibrium. Comparison of theory with experiment in this field absolutely demands constant awareness of the ubiquity of metastable defects in real CIS materials and thus great caution when generalizing limited experimental data.

The starting point for atomistic analyses of the defect chemistry of $CuInSe_2$ is the paper by Groenink and Janse[74] in which they outline a generalized approach for ternary compounds based on elaboration of an earlier model developed specifically for spinels by Schmalzried.[75] The number of arbitrary combinations of lattice point defects (vacancies, antisites, and interstitials) in a ternary system is so great that useful insight can only be gained by some approximation. Antisite defects created by putting anions on cation sites or *vice versa* are reasonably neglected because of their extremely high formation energy. The requirement that the crystal as a whole is electrically neutral also leads naturally to Schmalzried's assumption that for any given combination of the thermodynamic variables the concentrations of some pair of defects with opposite charge deviation will be much higher than the concentrations of all other defects. Groenink and Janse referred to these as the "majority defect pairs". It is important to note that their treatment assumes that these pairs behave as noninteracting point defects, hence in this context these are "pairs" only in the sense that they occur in roughly equal numbers. It is also significant that this pair dominance implies that conduction processes in these materials might inevitability be characterized by significant electrical compensation, deep level ionized impurity scattering, or both.

The generalized approach by Groenink and Janse was applied specifically to I–III–VI_2 compounds by Rincón and Wasim,[76] who derived the proper form for the two parameters most useful for quantifying the deviation of the composition of these compounds or their alloys from their ideal stoichiometric values:

$$\Delta m = \frac{[I]}{[III]} - 1 \qquad \textit{molecularity deviation}$$

$$\Delta s = \frac{2 * [VI]}{[I] + 3 * [III]} - 1 \qquad \textit{valency deviation}$$

Note that in the notation employed in these equations [I], for example, denotes the Group I atom fraction. Inasmuch as [I]+[III]+[VI]=1, these two deviation variables uniquely specify the solid solution composition.

In the same way that a sum rule enables the composition of any ternary mixture to be specified completely using only two of its three fractional compositions, the composition can alternatively be specified by the two variables Δm and Δs. They are coordinates within the ternary I–III–VI composition triangle of the point corresponding to a compound's actual composition in a coordinate system whose origin is at the point of I–III–VI_2 stoichiometry and whose axes are along (molecularity) and transverse (valency) to the I_2VI–III_2VI_3 section. Within the composition range where the I–III–VI_2 compound or alloy remains single phase, these variables may be properly viewed as analogous to the "normal coordinates" of a dynamical system in the Lagrangean formulation of the physics of motion. This coordinate system's molecularity axis is the fixed segment connecting Cu_2Se and In_2Se_3 on the boundaries of the ternary composition triangle, but the valency axis crosses it at an angle that varies such that it always connects to the selenium vertex. Rincón and Wasim[76] have analyzed the defect behavior of CIS in the region around stoichiometric $CuInSe_2$, which shows that the 18 ionized point defects allowed in these approximations yield 81 ($= 9 * 9$) "majority defect pairs", and which might dominate in each of the four quadrants or at their boundaries. It is argued subsequently in this section that those conclusions are in part erroneous because their analysis does not consider point defect complexes.

The merit of molecularity and valency deviations as intrinsically relevant composition measures in CIS has been demonstrated empirically by careful studies of conductivity in single crystal $CuInSe_2$.[7] Neumann and Tomlinson demonstrated that within the range $|\Delta m| < 0.08$ and $|\Delta s| < 0.06$, *p*-type conductivity occurs whenever $\Delta s > 0$ (electron deficiency), whereas *n*-type conductivity occurs for $\Delta s < 0$ (electron surplus). Their Hall effect measurements also showed that the dominant acceptor changed in *p*-type CIS from shallow (20 to 30 meV) whenever $\Delta m > 0$ (excess copper) to deeper (78 to 90 meV) when $\Delta m < 0$ (indium rich).

The actual predominance of a specific majority defect pair in any given quadrant of the molecularity vs. valency domain will in equilibrium be determined by whether its free energy is lower than that of the other probable pairs. A vast amount of theoretical analysis[77-79] was directed in the 1980s toward estimation of the enthalpies of the formation of the various point defects because their experimental determination is formidable. There is clear agreement among those analyses that the energy of formation for an isolated point defect is lowest for the cation antisite defects Cu_{In} and In_{Cu}. There was some disagreement as to whether the next lowest formation enthalpy values are for the copper vacancy, V_{Cu},[77,79] or selenium vacancy, V_{Se}.[78]

There remained several disturbing issues with those analyses. First is the lack of the predicted correlation between the composition and net carrier concentration.[7] Second is the low level of minority carrier recombination in polycrystalline CIS PV devices, which are always made with significant negative molecularity deviation, often in the biphasic $\alpha+\beta$ domain. Recalling that the chalcopyrite unit cell contains 16 atoms, a defect concentration of little more than 6% would yield a statistical probability of one defect per unit cell if they are distributed randomly.

Defect complexes provide a resolution of these deficiencies, as all the atomistic models described above exclude defect complexes (associates), which should be anticipated given the Coulombic attraction between the oppositely charged members of these "majority defect pairs". The dominant cohesive bonding force leading to the negative contribution to enthalpy that stabilizes ionic

crystals is the Madelung energy[80] resulting from precisely this Coulombic attraction. Furthermore, defect clustering and the resultant short-range ordering has been shown essential to understanding the defect chemistry of nonstoichiometric transition metal oxide phases.[64]

Theoretical *ab-initio* quantum-mechanical calculations of cation defect and defect complex formation enthalpies in $CuInSe_2$[81] recently have provided support for these assertions. These results showed that the formation enthalpies of lattice defects depend on the chemical potential of the constituent atomic species, and in the case of charged defects, on the chemical potential for electrons (equal to the Fermi energy at T = 0 K). The results showed explicitly that when the chemical potential of indium sufficiently exceeds that of copper the formation enthalpy of the $(In_{Cu}^{2+} + 2V_{Cu}^{-})^0$ neutral defect complex (NDC) actually becomes negative (energetically favorable). The formation of this defect requires the removal of three monovalent copper ions and substitution on one of those vacancies of the trivalent indium; hence, it has no net effect on the valence stoichiometry deviation Δs. Their calculations of the energetic effects of long-range ordering of the $(In_{Cu}^{2+} + 2V_{Cu}^{-})^0$ complex[82] showed that the reported compositions of indium-rich compounds ($\Delta m < 0$) on the pseudobinary section could be achieved by mathematically rational ratios of the numbers of this complex to the number of chalcopyrite unit cells, and that ordering was energetically favorable.

Additional long-range crystallographic ordering possibilities for the $(In_{Cu}^{2+} + 2V_{Cu}^{-})^0$ NDC have been proposed by Rockett,[83] and further investigations are needed to determine the true nature and extent of NDC ordering. Nevertheless, a recent study of the β-phase compound $CuIn_3Se_5$ (X = 0.75 in Figure 1)[49] has shown that the EXAFS scattering spectrum of selenium in this compound is best fit by a local structure model having precisely these defect proportions in the nearest-neighbor tetrahedra surrounding Se atoms in the lattice (Figure 2(c)). This is strong experimental evidence that the accommodation of excess indium on the lattice in CIS compounds on the pseudobinary section results in formation of this cation NDC.

Deviations from valence stoichiometry off the pseudobinary section ($\Delta s \neq 0$) cannot be caused by the $(In_{Cu}^{2+} + 2V_{Cu}^{-})^0$ NDC. Deviations of $\Delta s < 0$ are caused by defects that create an excess of electrons compared with those required to form the "normal valence compound".[84] As examples, an In_{Cu} antisite defect brings two more valence electrons to that lattice site than when normally occupied by copper (Cu_{Cu}); and V_{Se} creation removes two bonding orbitals from the lattice, which otherwise would be normally occupied, thereby freeing two electrons to be donated to the conduction band by cations. Conversely, deviations of $\Delta s > 0$ are caused by defects that create a deficiency of electrons needed for the normal valence configuration (e.g., V_{Cu}). These considerations led to the notation In_{Cu}^{2+}, which represents an In^{+3} ion placed at a cation antisite on the lattice that is normally occupied by Cu in its +1 oxidation state.

One of the other results from Zhang and co-workers' studies of cation defect energetics in CIS is their calculation of electronic transitions associated with the ionization of isolated point defects and clusters.[81] Their quantum-mechanical studies show that the disparity between relative ionicity and covalency of the copper and indium bonds, respectively, result in an unexpectedly shallow acceptor level for V_{Cu} (30 meV) and unexpectedly deep donor levels (E_c-0.24 and E_c-0.59 eV) for the indium cation antisite, In_{Cu}. The shallow donor seen in α–$CuInSe_2$ with deviations of $\Delta s > 0$ had been attributed in many studies to In_{Cu} acting as a donor, but these results show that both of its ionization levels are deeper than that of the $(In_{Cu}^{2+} + V_{Cu}^{-})^+$ part of the NDC and all were too deep to correspond to the very shallow (20 to 30 meV) donor seen in numerous studies.[7]

One of the limitations of Zhang and co-workers' earlier studies of cation defect energetics in CIS was neglect of defects on the anion sublattice. In particular, the V_{Se} is another widely suggested candidate for this shallow donor defect.[7,79,85] More recent *ab-initio* quantum-mechanical calculations of the $V_{Se} \rightarrow V_{Se}^{+2}$ electronic transition energy[86]

predict that significant lattice relaxation is associated with the V_{Se} ionization process, and that the energy level of the indirect (phonon-assisted) transition is E_c-0.1 ± 0.05 eV. This represents the most shallow donor level calculated for any of the point defects investigated theoretically by that group.

Investigations of vacancy defects in epitaxial $CuInSe_2$/GaAs via positron annihilation lifetime studies have been interpreted to suggest that the most probable defect is the $(V_{Se} + V_{Cu})$ defect.[87-89] The possible role of V_{Se} and cation-anion point-defect complexes in CIS with negative deviations from valence stoichiometry (i.e., off the pseudobinary section with $\Delta s < 0$) does not yet appear to have been resolved. Van Vechten has argued[90] that V_{Se} is unlikely to be stable in indium-rich materials, proposing a defect annihilation mechanism when both $\Delta m < 0$ and $\Delta s < 0$ based on the quasichemical reaction:

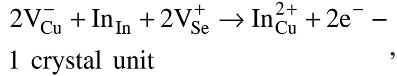

$$2V_{Cu}^{-} + In_{In} + 2V_{Se}^{+} \rightarrow In_{Cu}^{2+} + 2e^{-} - 1 \text{ crystal unit},$$

which he suggests would be energetically favorable because of the large cohesive energy of the lattice compared to the energy of In_{Cu} formation.

C. Optical Properties of Ternary Cu–III–VI Compounds

The first subsection herein describes the ubiquitous phenomenon of composition-dependent optical properties found in this class of compounds, within the finite extent of their respective single-phase domains. The focus of the remainder of this section is the fundamental optical bandgaps of the α-phase compounds $CuInSe_2$, $CuInS_2$, $CuGaSe_2$, and of their associated β-phases. Discussion of the opto-electronic properties of alloys of these compounds are deferred to the following section.

1. Variation of Optical Absorption with Composition

The fundamental absorption edge for intrinsic undoped semiconductors can be determined by extrapolation of the plot of the absorption coefficient α vs. $\sqrt{h\upsilon}$ to $\alpha = 0$.[91] Residual absorption at energies below the fundamental absorption edge in semiconductors that obeys the empirical relationship $d(\ln \alpha)/d(h\upsilon) = 1/kT$ is referred to as an Urbach tail.[92] This is known in conventional extrinsically doped semiconductors to arise via the Franz-Keldysh effect produced by spatial fluctuations of the internal electrostatic field to give spatial variations in charged impurity density[93] over distances larger than the Debye screening length. Photon-assisted tunneling[94] between the resulting exponential bandtails[95] results in these characteristic exponential optical absorption tails.

The temperature and spectral dependence of the observed sub-bandgap absorption in single crystal $CuInSe_2$ has been studied carefully by Nakanishi and co-workers.[96] When they fit their data to the conventional equation[97] of the Urbach form:

$$\alpha = \alpha_0 \exp\left[\frac{\sigma(h\upsilon - E_0)}{kT}\right],$$

where, with $\hbar\omega_p$ representing the optical phonon energy [98]:

$$\sigma = \sigma_0\left(\frac{2kT}{\hbar\omega_p}\right)\tanh\left(\frac{\hbar\omega_p}{2kT}\right),$$

they found that unphysically large values for the optical phonon energy were required, and that they depended on composition. However, using the equation:

$$\alpha = \alpha_0 \exp\left[\frac{(h\upsilon - E_0)}{E_a(T,x)}\right],$$

they separated $E_a(T,x)$ into the sum of two terms, one linearly dependent on composition and the other a temperature-dependent factor that fit the prior two equations with the reported value for the optical phonon energy. They concluded that the exponential optical absorption bandtails in $CuInSe_2$ arise both from phonon and compositional fluctuations, the latter increasing linearly with negative molecularity deviation.

Further variations in optical absorption and emission of α-CIS are associated with negative valence stoichiometry deviations ($\Delta s < 0$). Early annealing studies[85] showed a significant red-shift of photoluminescence emission when bulk samples were annealed or synthesized in excess indium vapor, and a reversible blue-shift after synthesis or annealing in excess selenium vapor. A more recent study[99] suggests the formation of an impurity (V_{Se}) subband when $\Delta s < 0.05$.

This phenomenon of strong sub-bandgap absorption in indium-rich CIS giving rise to apparent narrowing of the effective bandgap is also observed in epitaxial films of CIS on GaAs studied by piezoelectric photoacoustic spectroscopy,[100] evidence that it is a consequence of the native defect structure of these materials, and not an artifact of polycrystallinity, preparation, or measurement technique. It appears that this effect extends to the biphasic α–β composition domain, which suggests that the coexistence of these two phases is accompanied by an interaction between them that results in composition fluctuations manifested as strong band-tailing in their combined optical absorption. It is unclear whether this is predominately an equilibrium phenomenon or related to ubiquitous metastable defect structures common to the materials investigated by so many researchers.

2. Lattice Dynamics and Infrared Optical Properties

The symmetry properties of the chalcopyrite structure's phonon modes are described by the irreducible representation of its corresponding $I\bar{4}2d$ space group,[101] which yields 21 fundamental modes:

$$\Gamma_{opt} = 1\ A_1 + 2\ A_2 + 3\ B_1 + 3\ B_2 + 6\ E.$$

All of these modes except the A_2 are Raman active. Their frequency assignments for $CuInSe_2$ are provided in the comprehensive study of single crystals by Tanino et al.[102] The phonon mode structure of many other α-phase copper ternary chalcopyrite compounds have been studied in detail, including $CuGaSe_2$;[103] $CuInS_2$;[104] and $CuGaS_2$.[105,106] In addition, the Raman spectra of the β-phase compounds $Cu_2In_4Se_7$,[107] $CuIn_3Se_5$,[108] and $CuGa_3Se_5$[109] have been reported. The dominant A_1 Raman mode of the corresponding α-phase compound for each of these β-phase compounds is found to shift to smaller wavenumbers. Because the A_1 mode involves only anion displacement, with the cations at rest, this shift has been attributed to a weakening of the force constants coupling the anions to the lattice by the prevalence of cation vacancies in the β-phase.[110] Finally, the phonon structure of the CuAu crystallographic polytype of $CuInSe_2$ has been published recently.[72]

3. Optical Properties of α–CIS and β–CIS

Early measurements of the bandgap energy of single-crystal $CuInSe_2$ exhibited nominal discrepancies,[111,112] suggesting a value in the range of 1.02 to 1.04 eV. Subsequent studies[113,114] showed evidence of significant optical absorption at energies below this fundamental absorption edge. Characterization of polycrystalline CIS absorber films suitable for devices almost always indicate a significantly lower effective bandgap of ~0.90 eV,[115] apparently a consequence of significant collection of carriers generated by absorption in these band-tails. It has been suggested that the widely reported variations in the optical properties of CIS materials are a direct consequence of variations in composition.[116]

The most recent published study of radiative recombination in near-stoichiometric $CuInSe_2$ epilayers on GaAs yields a value for the fundamental absorption edge of E_g = 1.046 eV at a temperature of 2 K, with a slight increase to a value of E_g = 1.048 eV at a temperature of 102 K.[117] Near room temperature, however, the temperature dependence follows the Varshni relation:[118]

$$E_g(T) = E_g(0) - \frac{\alpha T^2}{T + \beta}$$

with $\beta = 0$ and $\alpha = 1.1 \times 10^{-4}\, eV / K$.[116]

Anomolous low-temperature absorption edge dependency is often observed in of I–III–VI_2

semiconductors.[119] This phenomenon is discussed in further detail in the section describing the optical properties of $CuGaSe_2$, as it has been investigated more thoroughly for that compound.

This low- and high-temperature data published by Nakanishi and co-workers[116] was subsequently fitted over the entire temperature range[120] to the Manoogian-Lecrerc equation:[121]

$$E_g(T) = E_g(0) - UT^s - V\left[\coth\left(\frac{\phi}{2T}\right)\right].$$

The fitting parameters $E_g(0)$, U, V, and s are temperature-independent constants, although they do have relevant physical significance. For example, the second and third terms represent the effects of lattice dilation and electron-phonon interactions, respectively. The temperature ϕ is the Einstein temperature, related to the Debye temperature by $\phi \cong \frac{3}{4}\phi_D$,[120] and the value used in their calculations was derived from the published value of $\phi_D = 225\ K$,[122] yeilding $\phi = 170\ K$. The best fit to that data was found for

$$E_g(0) = 1.036\ [eV]$$
$$U = -4.238 \times 10^{-5}\ \left[eV \cdot K^{-1}\right],$$
$$V = 0.875 \times 10^{-4}\ \left[eV \cdot K^{-1}\right], \text{ and s = 1.}$$

The corresponding 300 K bandgap energy is 1.01 *e*V. Note the ~10 m*e*V discrepancy between this value for the bandgap at absolute zero temperature and that discussed earlier in this section.[117]

The spectral dependence of the refractive index of $CuInSe_2$ has been reported for both bulk and polycrystalline[123] materials as well as epitaxial films on GaAs.[124] Here, too, significant discrepancies are found in the reported data.

Analogous discrepancies are found in the reported optical properties of β-CIS synthesized by different techniques. Polycrystalline films with an overall composition corresponding to the compound $CuIn_3Se_5$ are reported to exhibit a room-temperature fundamental absorption edge at 1.3 eV.[58] Optical absorption and cathodoluminescence characterization of heteroepitaxial $CuIn_3Se_5$ films on GaAs has been interpreted to indicate a bandgap of $E_g \geq 1.18$ eV at 8 K.[125] The most thorough characterization has been conducted on bulk polycrystalline samples with a nominal composition of $CuIn_3Se_5$.[126] The temperature dependence of the absorption coefficient edge was fitted using the Manoogian-Lecrerc equation. The best fit to their data was found for

$$E_g(0) = 1.25 - 1.28\ [eV],$$
$$U = 2.0 \times 10^{-5}\ \left[eV \cdot K^{-1}\right],$$
$$V = 1.2 - 1.5 \times 10^{-4}\ \left[eV \cdot K^{-1}\right],$$
$$\phi = 205 - 213\ [K], \text{ and s = 1.}$$

The corresponding 300-K bandgap energy is in the range of 1.19 to 1.21 eV. Although there are significant quantitative discrepancies between the various published data, they all agree without exception that the bandgap energy of β-CIS is substantially (0.2 to 0.3 *e*V) greater than that of α-CIS.

4. Optical Properties of α–CGS

The temperature dependence of the bandgap energy of $CuGaSe_2$ has been well characterized recently,[120] with the data also fit to the Manoogian-Lecrerc equation. The best fit to the data with s = 1 was found for

$$E_g(0) = 1.691\ [eV],$$
$$U = -8.82 \times 10^{-5}\ \left[eV \cdot K^{-1}\right], \text{ and}$$
$$V = 1.6 \times 10^{-4}\ \left[eV \cdot K^{-1}\right], \text{ with } \phi = 189\ K,$$

based on the reported Debye temperature for $CuGaSe_2$ of $\phi_D = 259\ K$.[122] The corresponding 300-K bandgap energy is 1.65 *e*V. Refractive index data for $CuGaSe_2$ over the range 0.78 to 12.0 μm has been reported by Boyd and co-workers.[127]

5. Optical Properties of α–CISU

The most recent determination of the bandgap of α–CISU was based on bulk two-phase Cu_xS + $CuInS_2$ samples with slight negative valence stoichiometry deviations analyzed by means of photoreflectance spectroscopy, yielding a value of 1.54 eV at 80 K.[128] Earlier measurements of the bandgap varied by about 30 meV in the range of 1.52 to 1.55 eV at room temperature.[129] The relationship of the effective bandgap to composition, discussed in the preceding CIS part of this section, was studied,[130] and the variance between previously published values was attributed to the same effect. In particular, a decrease in the effective bandgap was observed for negative valence stoichiometry deviations ($\Delta s < 0$).

The temperature dependence of the $CuInS_2$ bandgap is reported to exhibit anomalous low-temperature behavior, like that described for all the other Cu ternary chalcogenides discussed in this section.[131,132] Refractive index data for $CuInS_2$ over the range 0.9 to 12.0 μm has been reported by Boyd and co-workers.[133]

D. Alloys and Dopants Employed in CIS Photovoltaic Devices

A later section of this review describes in detail the reasons that most CIS PV devices are not made from the pure ternary compounds, but rather alloys thereof. Breifly, bandgap engineering is the principal motivation.[134] The nomenclature might be somewhat confusing in this section unless the reader keeps clearly in mind the distinction between a compound and an alloy. $CuInSe_2$, for example, is a ternary compound, as is $CuGaSe_2$. Both of these compounds show a small range of solid solution extent. An alloy of these two ternary compounds is a pseudobinary alloy, although it is also a quaternary material (it contains four elements). One may view this to first order as simple mixing of Ga on the In sublattice in α-CIS. By induction, mixture of that psuedobinary alloy, $Cu(In,Ga)Se_2$, with the ternary compound $CuInS_2$ yields the pseudoternary alloy $Cu(In,Ga)(S,Se)_2$, which is also a pentanary material.

1. Gallium Pseudobinary Alloy — CIGS

Until the very recent publication of the dissertation of Dr. Cornelia Beilharz,[135] no comprehensive thermochemical study of the quaternary CIGS phase field was available. This is remarkable in view of the fact that most of the published world record thin film solar cell efficiencies since 1987 (and all since 1995) have been held by CIGS-based devices. The predominant phase fields in the pseudoternary Cu_2Se–In_2Se_3–Ga_2Se_3 composition diagram as reported in that work are shown Figure 4.

The most obviously important aspect of this CIGS pseudoternary predominance diagram is the monotonic broadening of the α–CIGS single-phase domain toward more Group III-rich compositions with increasing Ga. Practically speaking, this means that synthesis of single α–phase CIGS requires less precise control over the [I]/[III] ratio (molecularity) than needed for single phase α–CIS synthesis, irrespective of the technique employed. Secondly, the appearance of a domain characterized by both α– CIGS (designated Ch in Figure 4) and β–CIGS (designated P1 in Figure 4) plus the disordered zincblende (Zb) structure, not found at room temperature in either of the pure ternary compounds. Note that the extent of this domain (designated Ch+P1+Zb in Figure 4) along lines of constant [In]/[Ga] molar ratio (i.e., lines emanating from the Cu_2Se corner) is minimal in precisely the composition range around 25% gallium where the highest efficiency CIGS devices are fabricated.[136,137]

A theoretical study of the effects of gallium addition to $CuInSe_2$ provides some insight into likely atomic-scale phenomena leading to these effects.[138] Wei and co-workers calculate that the energy of formation for the isolated group III cation antisite defect, Ga_{Cu}, is 0.2 to 0.9 eV greater (depending on its ionization state) than that of In_{Cu}. Also, they calculate that the donor levels for isolated Ga_{Cu}, are deeper than those of In_{Cu}, hence if present in comparable concentrations Ga_{Cu} will not thermally ionize as easily as In_{Cu}, and therefore contribute less to compensation of the acceptors that must dominate for *p*-type conductivity to prevail. Note that the applicability of this reasoning is moderated to the extent that the donors and

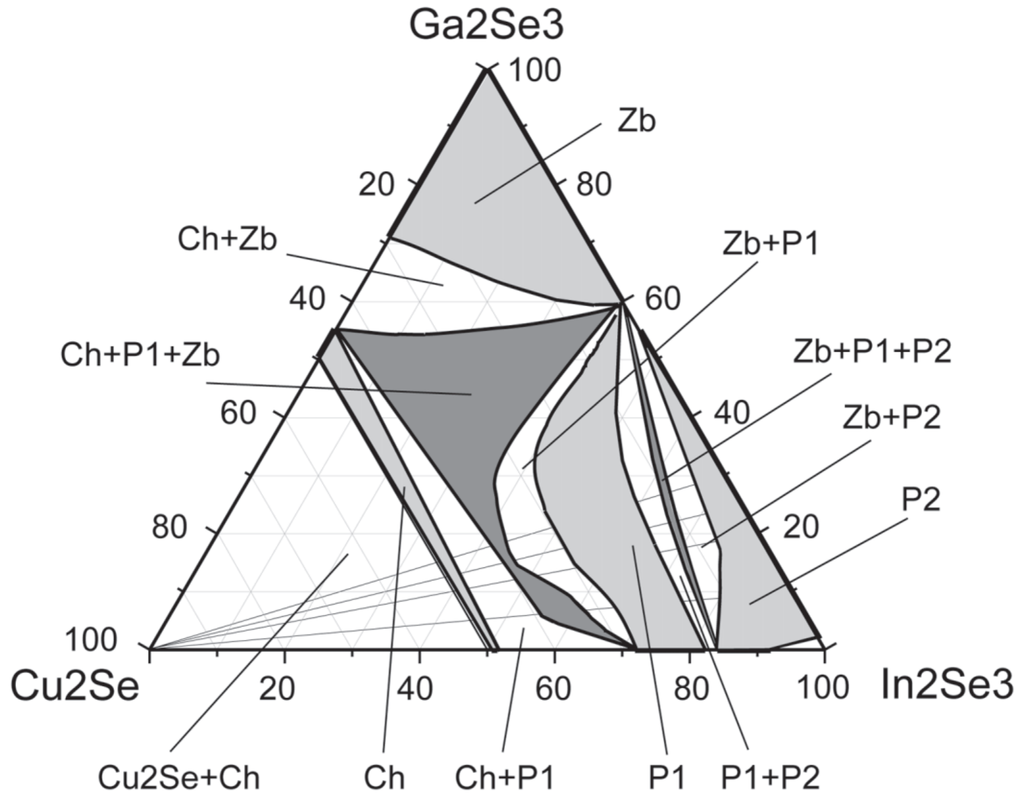

FIGURE 4. Predominance diagram for the Cu_2Se–In_2Se_3–Ga_2Se_3 pseudoternary phase field at room temperature.[135] In that author's notation, Ch is the α phase, P1 is the β phase, P2 is the γ phase, and Zb is the δ phase.

acceptors are within tunneling lengths of one another, in which case thermal ionization is not required for charge exchange to occur. Nevertheless, it is consistent with the experimental observation that hole densities are higher in CIGS epitaxial films than in CIS epitaxial films with comparable molecularity and valence stoichiometry.[139] Finally, the $(Ga_{Cu}^{2+} + 2V_{Cu}^{-})^0$ Neutral Defect Complex (NDC) is calculated to require 0.4 eV more energy to form than the $(In_{Cu}^{2+} + 2V_{Cu}^{-})^0$ NDC, leading to 0.3 eV higher formation energy per NDC in the Ordered Defect Compounds (ODC) (i.e., β or P1 phase) containing gallium. This suggests that in CIGS materials with negative molecularity deviation, under conditions where NDC aggregation can occur, ODC formation is more energetically favorable in regions where composition fluctuations have led to a lower local gallium concentration.

2. Bandgap Dependence on CIGS Composition

Alloys of the copper ternary chalcopyrite compounds, like those of virtually all the zincblende binary alloys, are found to exhibit a sublinear dependence of their bandgap energy on alloy composition. Their functional relationship is well approximated by the expression:

$$E_g(x) = xE_g(1) + (1-x)E_g(0) - b(1-x)x\,,$$

where the parameter b is referred to as the "bowing parameter". Optical bowing is now understood to be a consequence of bond alternation in the lattice.[47] Free energy minimization results in a tendency for A and B atoms to avoid each other as nearest neighbors on the cation sublattice in

$A_xB_{1-x}C$ alloys, resulting in short-range ordering referred to as anticlustering.[140,Chapter 4]

A very large range of bowing parameters has been reported for CIGS thin films and bulk $Cu(In,Ga)Se_2$, varying from nearly 0 to 0.25, and data on thin film CIGS absorber layers strongly supports the contention that this variability is a consequence of variations in molecularity deviation between the samples reported by various investigators.[141, and reference therein] Another study of combined temperature and composition dependencies of the bandgap in bulk crystalline $Cu(In,Ga)Se_2$ concluded that the bowing parameter may be temperature dependent.[120] A theoretical value of 0.21 at absolute zero has also been calculated.[138] A preponderance of the room temperature data are in the range of 0.14[142] to 0.16,[143] so the intermediate value of $b = 0.151$ from the original work by Bodnar and co-workers is accepted here,[144] leading to the following expression for α–$CuIn_{1-X}Ga_XSe_2$:

$$E_g^{CIGS}(x) = 1.65x + 1.01(1-x) - 0.151(1-x)x$$

3. Sulfur Pseudobinary Alloy —CISS

Woefully little thermochemical and structural data are available for the Cu–In–Se–S quaternary system. The bandgap dependence on composition has been reported by several researchers, with the reported optical bowing parameters varying from 0 to 0.88.[145-147] There is substantially better agreement between a larger number of studies of the mixed-anion alloy $CuGa(Se_XS_{1-X})_2$ that the optical bowing parameter in that system is zero.[148, and references therein] It has been argued that the bond-alternation, which leads to optical bowing in mixed-cation ternary chalcopyrite alloys, does not occur in the mixed-anion alloys,[149] and that the bowing parameter therefore should vanish in $CuIn(Se_XS_{1-X})_2$, as reported by Bodnar and co-workers.[145] The substantial uncertainty and disagreement among the published experimental results suggests that resolution of this question will require further investigation.

4. Alkali Impurities in CIS and Related Materials

The importance of sodium for the optimization of polycrystalline CIS thin-film solar cell absorber layers has been studied extensively since first suggested by Hedström and co-workers.[150] Their careful investigation of the serendipitous sodium "contamination" of CIS absorber films due to exchange from soda-lime glass substrates contributed to their achievement of the first CIS device with a reported efficiency exceeding 15%. Subsequent studies have concluded that whether derived from the substrate[151] or added intentionally from extrinsic sources,[152-154] optimized sodium incorporation is beneficial to device performance, and excess sodium is detrimental.[155-158] Studies of sodium's concentration and distribution in the films show it is typically present at a ~0.1 at. % concentration,[159] and strongly segregates to the surface[160] and grain boundaries.[161]

A plethora of mechanisms has been suggested in an effort to explain the beneficial influence of sodium, and an overview of the body of literature taken together suggests that multiple effects contribute thereto. The primary phenomenological effects in CIS and CIGS absorber materials may be summarized as:

1. An increase in *p*-type conductivity[162] due both to the elimination of deep hole traps,[163] and an increase in net hole concentration resulting predominately from reduced compensation.[164]
2. An increase in the texture (predominance of uniaxial crystallite orientation) and the average grain size in polycrystalline films,[165] with a concomitant reduction in surface roughness.
3. An increased range of compositions (specifically negative molecularity deviations) that yield devices with comparable performance.[166-168]

These effects have been attributed to both direct and indirect electronic effects of sodium in the resulting materials themselves, and to the

dynamic effects of sodium during the synthesis process. These will be each discussed in turn, beginning with the one model that attributes the improved properties of absorbers that contain sodium on a bulk defect containing sodium.

Substitution of sodium for indium, creating residual Na_{In} antisite defect acceptors in the lattice of the resulting material, has been proposed to explain the observed increase in *p*-type conductivity.[159] Theoretical calculations predict[86] that its first ionization level, at 0.20 *e*V above the valence band edge, is shallower than that of Cu_{In}, but in typically indium-rich absorbers the formation of the Cu_{In} defect is less energetically favorable than are V_{Cu} and In_{Cu}, the structural components of the cation NDC. Furthermore, they calculate the formation enthalpy of the Na_{In} antisite defect is quite large (2.5 *e*V) when the compounds $CuInSe_2$ and $NaInSe_2$ are in thermal equilibrium.

The simplest indirect model for the sodium effect on conductivity is that the Na_{Cu} defect is more energetically favorable than the In_{Cu} defect, so it competes effectively for vacant copper sites during growth, thereby reducing the concentration of the compensating In_{Cu} antisite defect[169] in the resulting material.

A related model proposes that formation of Na_{Cu} substitutional defects in *lieu* of In_{Cu} is a transition state of the growth reaction in indium-rich materials, leading to a reduction in the final In_{Cu} antisite defect density within the bulk by inhibiting the incorporation of excess indium into the lattice.[170] In this model, sodium acts as a surfactant at the boundary between stoichiometric and indium-rich CIS, forming a two-phase $CuInSe_2$ + $NaInSe_2$ mixture or quaternary compound if sufficient sodium is available.[171,172] The advantages of this model are that it predicts a reduction in the concentration of In_{Cu} point defects and the NDC defect complexes in the bulk.[173] This model addresses all three of the primary sodium effects: the morphological changes are a surfactant effect, and the increased tolerance to negative molecularity deviation an electronic consequence of enhanced segregation of excess indium.

A study of the effects of elemental sodium deposited onto $CuInSe_2$ single crystals[174] led the authors to conclude that Na atoms at the surface disrupt Cu-Se bonds, releasing Cu^+ ions. These ions subsequently diffuse into the bulk under the influence of the surface field resulting from band-bending induced by the sodium itself, thereby increasing the concentration of V_{Cu} acceptors in the near-surface region. They also suggest that Na_{Cu} substitutional defects are created during this process. For high doses of sodium, they find that this lattice disruption results in the decomposition of $CuInSe_2$, yielding metallic indium and Na_2Se, and suggest that β–phase compounds may form at the surface as intermediate reaction byproducts due to the enhanced V_{Cu} concentrations. It is difficult to understand how these effects would increase *p*-type conductivity, because the excess copper ions released from the surface and driven into the bulk would most likely recombine with the V_{Cu} shallow acceptors that make it so.

Two other models attribute the influence of sodium on electronic properties to its effects on the concentration of selenium vacancies. The first of these[168] suggests that sodium at grain boundaries catalyzes the dissociation of atmospheric O_2, creating atomic oxygen that neutralizes surface V_{Se} by activated chemisorption, leading to the formation of a shallow acceptor.[175,176] Theoretical calculations of the bulk O_{Se} ionization energy level predict very deep levels,[86] however, and studies of the electronic influence of implanted and annealed sodium in epitaxial $Cu(In,Ga)Se_2$ films provide evidence for substantially reduced compensation without any evidence of oxygen diffusion into the bulk.[164]

The final published model for the effects of sodium attributes its influence to increased chemical activity of selenium at the film's surface during growth.[177] Strong evidence is provided that sodium polyselenides (Na_2Se_x) form on the surface during growth, and they suggest that this acts as a "reservoir" for selenium on the surface, reducing the formation of compensating V_{Se} donor defects. Reduced compensation resulting from combined selenium and indium enrichment of the α–CIS lattice is also predicted by this author's statistical thermodynamic calculations,[37] although the defect mechanism is reduced concentration of the $(In_{Cu}^{2+} + V_{Cu}^{-})^{+}$ defect complex (NDC dissociation fragment) rather than that of V_{Se}. This is discussed further in the next section.

E. Electronic and Ionic Transport in CIS Photovoltaic Device Materials

Clearly, the distinguishing characteristic of the CIGSS family of materials when compared with conventional semiconductors is its plethora of crystal structures and phases, none of which can be characterized as line compounds. The ability of even pure single phases of these materials to accommodate intrinsic crystallographic defect concentrations, particularly vacancies, on the order of 1% (~ $10^{20}/cm^3$) without decomposing is completely different than the behavior of the Group IV and almost all III-V compound semiconductors. Not surprisingly, this results in electronic transport properties that often cannot be modeled using theories based on simplifying assumptions that are inappropriate to such highly disordered materials. Even one of the most basic assumptions made in conventional semiconductors, that electronic and ionic transport are decoupled, does not apply under some typical circumstances. Consequently, more complex models that borrow concepts from the theories of disordered materials and electrochemistry must be employed to understand the behavior of CIGSS photovoltaic devices.

1. Electronic Carrier Concentration and Composition

As mentioned in a preceding section, single crystal $CuInSe_2$ studies by Neumann and Tomlinson[7] showed that within the range $|\Delta m| < 0.08$ and $|\Delta s| < 0.06$, *p*-type conductivity occurs whenever $\Delta s > 0$, whereas *n*-type conductivity occurs for $\Delta s < 0$. Their Hall effect measurements also showed that the dominant acceptor changed in **p**-type CIS from shallow (20 to 30 meV) whenever $\Delta m > 0$ to deeper (78 to 90 meV) when $\Delta m < 0$. Their statistics in support of these general conclusions were excellent (176 samples), but it should be noted that insufficient data were reported to establish that the exact value of the transition from a shallow to deep acceptor for $\Delta s > 0$ was precisely $\Delta m = 0$. They found no as-grown samples with both $\Delta m < 0$ and $\Delta s > 0$ so they annealed five samples with $\Delta m < 0$ and $\Delta s < 0$ in selenium, which moved their compositions into the $\Delta m < 0$ and $\Delta s > 0$ quadrant of the molecularity vs. valency domain, and which changed their conductivity from n-type to p-type.

Neumann and Tomlinson assigned the shallow ($E_c - E_d < 20$ meV) donor responsible for *n*-type conductivity in all their samples with $\Delta s < 0$ to two possible intrinsic point defects, the selenium vacancy V_{Se} or the indium antisite In_{Cu}. Recent first-principle quantum-mechanical calculations of the electronic transition levels of these two defects[81,86] suggest that the indium antisite ionization transition yields an electronic level too deep in the bandgap to correspond to the observed shallow donor. The indirect selenium-vacancy ionization transition on the other hand could yield the shallow donor level observed in CIS with negative stoichiometry deviation.

Neumann and Tomlinson assigned the shallow acceptor ($E_a - E_v \cong 20$–30 meV) leading to *p*-type conductivity in copper-rich samples ($\Delta m > 0$) to V_{In} and/or the copper antisite Cu_{In}. It is difficult to reconcile this conclusion with the results of recent thermodynamic studies,[31,34] which place the single-phase α–CIS/$Cu_{2-}\delta Se$ room-temperature boundary at $[Cu] = 24.5\%$, or equivalently $(\Delta m, \Delta s) = (-0.0316, 0)$. In equilibrium, any CIS sample with $\Delta m \geq -.03$ should be a two-phase mixture. This author suggests that those stoichiometric or copper-rich *p*-type samples that exhibited the shallow acceptor might have been either two-phase Cu_2Se +α–CIS mixtures or single phase α–CIS supersaturated with copper. $Cu_{2-}\delta Se$ is known to be strongly *p*-type,[178] and the previously described results of quenching studies[31] are consistent with the latter hypothesis.

For the indium-rich ($\Delta m < 0$) p-type samples created by annealing in selenium, Neumann and Tomlinson assign the deeper acceptor level that they found ($E_a - E_v \cong 78$–90 meV) to the copper vacancy V_{Cu}. This author recently developed

the first computational free energy defect model for $CuInSe_2$ that includes the effects of defect associates (complexes).[37] This model correctly predicts the change of dominant electronic carrier type in α-CIS with composition as reported by Neumann and Tomlinson within the uncertainty of their experimental data. However, this model predicts significant changes in the dominant defects and carrier type resulting from experimentally indistinguishable differences in selenium content of the pseudobinary Cu_2Se/In_2Se_3 section. The dominant defects on the binary are predicted to be V_{Cu} and the $V_{Cu} + In_{Cu}$ complex, which nearly compensate one another. The addition of as little as 0.08% excess selenium ($\Delta s = +0.004$) to the indium-rich ($\Delta m < 0$) α-CIS lattice is predicted to result in the conversion of the compensating $V_{Cu} + In_{Cu}$ donor complex to the Cu_{In} antisite, but in lower concentrations that do not significantly compensate the remaining V_{Cu} acceptors, yielding *p*-type α-CIS. Consistent experimental results are reported from studies of single-crystal CIS directly synthesized from indium-rich Cu/In alloys, which are *n*-type when formed under low and *p*-type under high selenium pressures.[179]

This author suggests that good quality CIS absorber films are slightly selenium enriched, which mitigates compensation of the dominant V_{Cu} acceptor by the mechanism described above, and that the excess indium in them is segregated into secondary phase β–CIS domains to differing extents,[170] which will strongly effect their carrier transport and recombination properties.[180]

2. Electronic Transport in CIS

The nonstoichiometric character of device-quality CIS and its alloys that are used to fabricate photovoltaic devices[181] has been emphasized in this article. A marginally detectable 0.1% atomic composition deviation from stoichiometry will induce in a single homogeneous phase total defect concentrations on the order of ~10^{19} cm^3. Coexistence with a minor secondary phase of different stoichiometry can reduce the effective stoichiometry deviation of the primary phase and thus the lattice defect concentration therein. Actual device materials typically possess easily measurable negative molecularity deviations an order of magnitude greater than the minimum experimentally resolvable.

Despite these total potential lattice defect concentrations of ~10^{20} cm^3, net carrier concentrations in CIS PV absorber films are typically ~10^{16-17} cm^3. It is apparent that there must either be nearly complete compensation or that only a small fraction of the total defect population can be electrically active (or both). There is experimental evidence for a modest density of neutral scattering centers (~ 5×10^{17}) in the analysis of temperature-dependent Hall effect measurements of epitaxial CIGS films with moderate negative molecularity deviation grown on GaAs.[139] It has been suggested that these neutral scattering centers might be the $(In_{Cu}^{2+} + 2V_{Cu}^{-})^0$ and/or $(Ga_{Cu}^{2+} + 2V_{Cu}^{-})^0$ cation neutral defect complexes.[83] the formation of which will accommodate negative molecularity deviation. However, short-range ordering of these defects is equivalent to β-CIS phase domain formation in a prominent model of that phase's structure.[37,82,170]

There is also evidence for significant carrier compensation in *p*–type indium-rich CIS. One of the most compelling studies of this effect by Nomura and co-workers was based on analysis of the Hall-effect overshoot behavior of single-crystal CIS synthesized under controlled selenium pressure,[182] wherein it is found that high selenium vapor pressures were required to yield in *p*–type indium-rich CIS. The Hall overshoot effect is a classic indicator of a heavily doped and highly compensated semiconductor,[183] and its behavior in *p*–type indium-rich CIS was shown by Nomura and co-workers to exhibit an unusual activated temperature dependence for compensating donor density. Evidence was also provided that the compensating donor density remains constant with increasing acceptor density up to the low to mid 10^{17} range, and rapidly increases thereafter. Similar net carrier concentration saturation behavior is widely observed in highly doped stoichiometric compound semiconductors, and recently has been shown to be a fundamental consequence of the onset of carrier degeneracy, which reduces the formation enthalpy of compensating native defects.[184,185]

A preceding section on the optical properties of CIS discussed the experimental evidence that increasing negative molecularity deviation lead to larger exponential optical absorption bandtails in $CuInSe_2$.[96] This observed relationship would result from potential fluctuations induced by composition fluctuations if it is assumed that composition fluctuations increase with negative molecularity deviation. The theoretical foundation for increased sub-bandgap absorption in heavily doped, highly compensated semiconductors due to the resulting potential fluctuations is well established.[186,187] Peculiar features in the predicted low-temperature electronic conductivity behavior of such systems (a "Coulomb gap" in the density-of-states[188,189] and variable-range hopping[190]) have been observed specifically in $CuInSe_2$ and $Cu(In,Ga)Se_2$.[139,191]

Further evidence of compositional fluctuations and high compensation is provided by the study of CIGS and CIS thin film temperature-dependent carrier transport and photoluminescence emission behavior.[192-194] Those studies show that the donor-acceptor-pair recombination model used conventionally to model the radiation recombination properties of lightly doped stoichiometric semiconductors, which relies on the assumption that the defect-state wavefunctions do not overlap,[195] is inapplicable to *p*–type indium-rich CI(G)S. Both the conductivity and optical emission properties could be modeled in this case using the theory of Efros and Shklovskii for highly compensated highly defective semiconductors,[196] although the characteristic length scale of fluctuations that effect the luminescence and those that effect the conductivity are quite different.

The theory of Efros and Shklovskii shows that even randomly distributed donor and acceptor levels give rise in the high-density limit to long-range fluctuating electrostatic potentials that result from the spatial localization of charge carriers and consequent loss of effective screening. This results in what Blakemore referred to as covariant fluctuations in the band potentials,[183] which leads to a sensitive dependency[197] of long-range free carrier transport (DC conductivity) on it effective topological connectedness, a mode of conductivity through inhomogeneous media referred to as percolation transport.[198] This author believes that *p*–type indium-rich CIS is not typically characterized by random ionized impurity distributions, a consequence of the tendency of the compensating defects to form complexes, some of which may aggregate to form crystallographically coherent secondary phase β–CIS domains.[83] Thus, the theoretical results of percolation threshold calculations for various lattice types that rely on the random distribution assumption[196,and references therein] cannot be employed directly to predict the composition of the semiconductor-insulator transition. Because β–CIS has a higher bandgap than α–CIS,[199] formation of such domains would lead to contravariant fluctuations in the band potentials[183] correlated with composition fluctuations. The effects of correlated impurity distributions on the spectral density of electronic states has been treated theoretically,[180] and shown to yield the same effect as a random distribution, but with a different relationship between the measured effect and the size scale of the fluctuations.

The recombination of electronic carriers is critical to the performance of PV and other minority carrier devices, and in stoichiometric semiconductor materials such as silicon or GaAs can be modeled quite well using Shockley-Read-Hall (SRH) statistics[200,201] so long as the concentration of extrinsic defects remains sufficiently small that they do not interact and can be treated as independent. However, even in these materials, at concentrations of ~ 10^{19} cm^3, the probability that the quantum-mechanical wavefunctions of randomly distributed lattice defects will begin to overlap becomes significant.[183] The Pauli exclusion principle results in level-repulsion that splits apart the energy levels of the interacting defects, transforming the discrete, degenerate energy level of a specific type of point defect in the dilute limit into a distribution of energy levels (an impurity band). The inadequacy of SRH statistics for modeling of recombination rates in the space-charge region of polycrystalline CIGS PV devices has been experimentally demonstrated by the analysis of temperature-dependent transport in them.[202] A tunneling-assisted recombination model correctly fits the empirical data; further evidence that interacting defects render conventional models based on the dilute approximation inapplicable to understanding carrier transport and generation-recombination in *p*–type (In,Ga)-rich CIGS.[203,204]

3. Electromigration of Copper in CIS

Historically, CIS was first investigated as a candidate material for thin film PV devices in an effort to solve a technological problem associated with its predecessor, Cu_2S. Copper sulfide thin film cells tended to fail under bias due to shunting, all of which occurred because of the formation of copper nodules within those films. From a thermochemical perspective, this represents phase decomposition of the compound into a two-phase mixture of $Cu_{2-\delta}S$ and nearly pure copper. Researchers suggested at that time that the addition of indium to the lattice might stabilize the crystal with respect to such decomposition,[115] which has proven true. Both $Cu_{2-\delta}S$ and $Cu_{2-\delta}Se$ are superionic conductors,[205] in which copper can diffuse easily, with very little driving force required. The addition of indium diminishes, but does not eliminate the mobility of copper on the lattice, even at room temperature.[206] This has led some researchers to characterize CIS as a "semionic" conductor.[207]

Recently, the consequences of this remnant ionic conductivity have been recognized as the most likely explanation for the widespread observation of copper depletion at the surface of device-quality CIS absorber films. The investigators who first observed this believed that device performance was improved by processes that formed a secondary (indium-rich) β-CIS phase layer at the surface of the absorber.[58] Subsequently, it has been shown that the properties of the copper-deficient surface layer on CIS absorber films are substantially different than those of the equilibrium β-CIS phase.[61] The latter authors hypothesized that field-induced migration of copper ions away from the free surface, driven by the field resulting from pinning of the Fermi level there, leads to the observed surface copper depletion. Their conjecture is consistent with the body of literature on field-enhanced electromigration of copper in CIS,[208,209] which without exception conclude that a vacancy mechanism is most likely. Analysis of photoemission from single-crystal $CuInSe_2$, $CuGaSe_2$, and $CuInS_2$ surfaces have also shown evidence that copper vacancy generation accompanies CdS emitter contact formation to those surfaces.[210] The role of copper electromigration in CIS photovoltaic devices is discussed further in a subsequent section of this article.

III. CIS PHOTOVOLTAIC DEVICES

Initially studied for its potential application as a photodetector material for optical fiber communications systems, CIS first received significant attention as a solar cell material in 1975.[211] $CuInSe_2$ became the fourth material system used to create any solar cell that exceeded the psychologically significant power conversion efficiency threshold of 10%, with Shay and Wagner's landmark report of 12% power conversion efficiency using an epitaxial CdS layer grown by MBE onto bulk single crystal wafers in 1975.[212] Rapid development of thin-film polycrystalline CIS devices followed,[115] and soon after Cu_2S became the first thin-film cell to break the 10% efficiency threshold,[213] CIS[214] and amorphous silicon[215] followed in a dead heat for second. The CIS announcement, however, included data demonstrating the intrinsic stability of CIS devices, which eventually led most investigators to abandon Cu_2S research in favor of CIS.

Although initially $CuInSe_2$ was the focus of most study, the optimal single absorber bandgap for terrestrial solar energy conversion had been established[216-218] to be in the range of 1.3 to 1.5 eV, substantially greater than the 1.04 eV value of $CuInSe_2$.[85] Hence, considerable effort has been invested in bandgap engineering of $CuInSe_2$ by alloying it with $CuAlSe_2$,[219,220,221] $CuGaSe_2$,[142] and/or $CuInS_2$.[222] The latter has also been investigated extensively as a pure ternary compound for solar cell applications as the bandgap of $CuInS_2$ is 1.54 eV.[128] On the other hand, $CuInSe_2$ and $CuGaSe_2$ as ternary compounds provide a nearly optimal bandgap pair for a dual-absorber tandem or cascade solar cell structure[223] because the latter has a bandgap of 1.68 eV.[224] Hence, the $Cu(Al,In,Ga)(S,Se)_2$ family of alloys (CAIGSS) provide an ideal range of optical absorption energies for solar cell applications.

The absorption coefficient is also extremely high in the $Cu–III–VI_2$ materials, exceeding 10^5

cm^{-1} over most of the visible spectrum. This is greater than that of any other semiconductor used for PV applications as seen in Figure 5. From the point of view of device optimization, the absorption coefficient also plays a crucial role in the choice of materials for the absorber layer of a PV device. Indeed the dimensionless parameter αL, where α is the absorption coefficient and L the minority carrier diffusion length, is an excellent first-order measure of the suitability of a semiconductor to PV device applications. This is a straightforward consequence of the fact that the photon absorption process at energies greater than the fundamental absorption edge of a semiconductor creates an electron–hole pair, which in order to perform work must be separated to prevent their recombination before electron injection into the external circuit load connected to the device. The product αL is thus a first-order measure of the probability that an electron-hole pair created in a material by photon absorption can diffuse apart before recombining.

Although α is to first order an intrinsic property of the material, L may be viewed as a variable dependent on defect structure, composition (intrinsic and extrinsic doping), and processing parameters, subject to material-specific intrinsic limits. This follows from the Einstein relation connecting the diffusion length L with the fundamental mobility limit, an intrinsic property determined by the curvature of the band structure at the quasi-Fermi level of the minority carriers, and their lifetime, which is highly dependent on processing-induced defect structures in any real semiconductor.

Minority carrier collection in a PV device may be divided conceptually (and mathematically to an excellent approximation) into two components,[226] one due to diffusion in the field-free region and the other due to field-assisted collection in the space-charge region (wherein transport does not obey the diffusion equation). Recombination of carriers generated in the depletion region may exhibit very complex dependence on a material's defect structure. Thus, devices can often be engineered to achieve high carrier collection efficiency even in cases of poor field-free carrier diffusion lengths.[227,228]

From the foregoing discussion it should be clear that although the optical properties of the Cu(In,Ga)(S,Se) family of materials is exceptionally well suited to solar cell applications, their electronic transport properties are equally important to their viability as useful materials for PV devices. Although only collection of carriers from the field-free region is directly dependent on the minority carrier diffusion length, the collection of all minority carriers is dependent on their effective mass. The very low effective mass of electrons in these copper ternary chalcogenides has been discussed in previous sections so we note here only the obvious conclusion that *p*–type absorber materials are superior for PV devices fabricated from these materials. The facts that the only known amphoteric ternary Cu–III–VI compounds are $CuInSe_2$ and $CuInS_2$ and that $CuGaSe_2$ is always *p*–type,[4] combined with the beneficial effects on electronically active defect structures of controlled alloying in the Cu(In,Ga)(S,Se) material system are fundamental reasons that this pentanary is particularly appropriate for PV devices.

A. CIS Photovoltaic Device Structures

A wide variety of theoretical mechanisms have been proposed for application to the condensed-state conversion of optical to electrical power, but only solid state photodiodes have yet achieved adequate broad-band conversion efficiency to be of practical value for solar power generation. Although front-wall configurations have been studied for CIS-related PV devices, only back-wall devices have achieved conversion efficiencies comparable to that of the dominant material used for solar power modules, which is crystalline silicon. In the back-wall configuration[229] incident light that generates collectible charge carriers must first pass through an *n*-type semiconductor emitter structure before being absorbed in the *p*-type CIS layer. Each photon absorbed by the CIS layer generates an electron-hole pair and

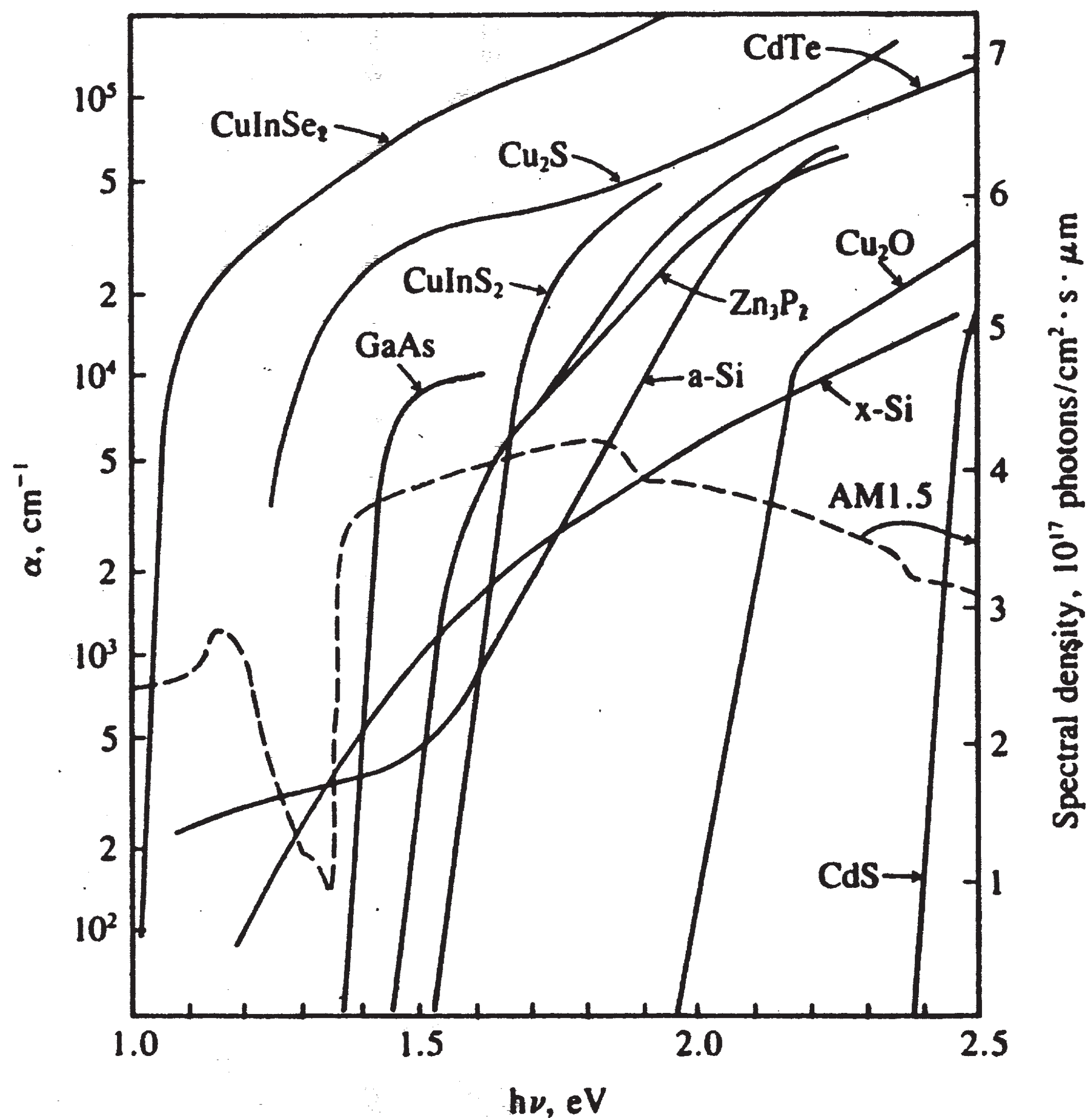

FIGURE 5. Optical absorption coefficient spectral dependence for various semiconductors.[225]

unless they recombine the hole transports to a backside metal contact while the electron injects across the diode's *p–n* junction into the emitter. The emitter invariably contains an n^+–n isotype junction to facilitate electrical contact and provide high lateral conductivity. Beyond this general description an enormous variety of materials and processes have been reported, which are detailed in the remainder of this section.

1. Absorber Structures

The complex crystallographic structure and phase composition of absorber layers made from this class of materials has been discussed in depth in the first half of this article. This subsection addresses the compositional, textural, and morphological properties of these films.

The constituent elements of CI(GS)S films produced by many methods are often completely redistributed within those films during their synthesis, unlike most conventional semiconductors. For example, whereas the III-V alloy (Al,Ga)As is usually grown with carefully tailored gradients in the relative composition of its constituent metal cations by modulating their relative fluxes during growth, in films of the alloy Cu(In,Ga)Se_2, copper, indium, and gallium typically redistribute during growth to create composition profiles in

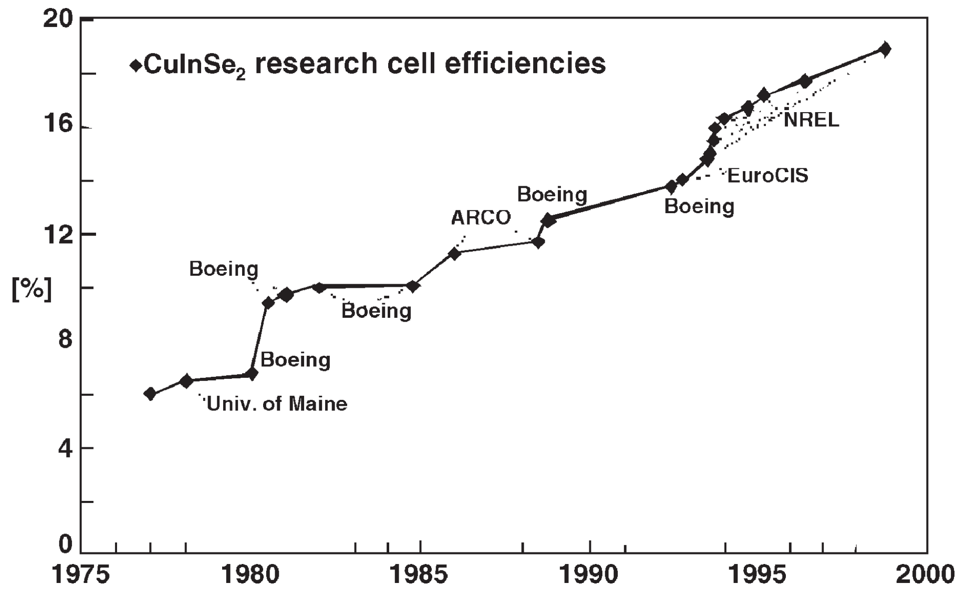

FIGURE 6. Progress in thin-film $CuInSe_2$ research cell efficiency, measured at STC (figure courtesy of L. Kazmerski, NREL.)

the final layers completely different from their initial distribution. This phenomenon is usually attributed to preferential segregation associated with the formation of transient secondary phases, but these intermediate reaction byproducts sometimes persist.

This persistence is commonly evident in CIGS layers, which often show evidence of multiple bandgaps and lattice constants, indicative of incomplete or inhomogeneous alloying of the constituent CIS and CGS ternaries.[230-232] Although this effect is sometimes unintentional and may be circumvented,[233] it has been exploited for the formation of graded-bandgap structures[234-236] intended to improve the performance of CIGS devices.[237,238] Likewise, the incorporation of sulfur into CIGS to form CIGSS absorbers[239] appears to be prone to strong interactions with both gallium[240] and copper[222] that can result in its nonuniform incorporation. There is evidence that the exchange of sulfur for selenium anions in the near-surface region of the absorber yields a reduction in recombination currents and thus higher device voltages.[158] This remains an active area of research.

On the other hand, gradients in copper composition seem to persist only at the surface of copper-deficient absorber films.[60] This subtle effect was not observed for many years, overshadowed by the more obvious disappearance of large (~30%) copper gradients between the first and second portions of the absorber synthesized by the Boeing bilayer approach.[241] The availability of excess copper during the initial film growth was found to yield much larger crystal grains in the final copper-deficient absorber film required for low majority carrier concentration.[242]

Another variable absorber layer property pertinent to device performance is its surface roughness. Simple photodiode theory[11] gives the open circuit voltage of an illuminated PV device as:

$$V_{oc} = A_0(kT/q)\ \ln((J_{sc}A_a/J_{00}A_t) + 1)$$

In this formulation the active (illuminated) area is A_a and the total area A_t. However, even in the case of uniform illumination and no grid shadowing, these areas can differ. This is because the inherent length scale for optical absorption is the absorption coefficient α, whereas the inherent length scale for recombination is the average distance between recombination centers. Because the latter is orders of magnitude smaller than the former, the active area is equivalent to the projected area while the total area is proportional to the contact area between the absorber and emitter. A microscopically rough junction increases the contact area but not the projected area, leading to lower voltages. Therefore, absorber layers with

smooth surfaces will yield higher voltage devices than those with otherwise identical material properties. Comparison of the formation of CIGS absorber films from $(In,Ga)_2Se_3$ and Cu-rich precursors have shown the relative smoothness of the former result in correspondingly smooth absorber films, with a lower ratio of surface to projected areas than the and Cu-rich precursor (Boeing) process.[243] The surface-smoothing influence of sodium impurities during growth[150] are also believed to improve device voltages in part because of this effect.[173]

The highest efficiency devices currently made have been shown to exhibit a different dominant crystallographic texture than earlier devices.[244] The constituent individual grains in all device-quality polycrystalline CI(GS)s absorber films are found to possess a high degree of preferred crystallographic orientation with respect to the substrate surface on which they are grown. This preferred crystallographic texture was historically found to yield {112} surfaces oriented parallel to the substrate surface,[150,245] and these surfaces are believed to be the lowest in energy when selenium terminated.[246,247] Current state-of-the-art absorbers are instead characterized by a {204} orientation, most likely a consequence of the direct transformation of the $(In,Ga)_2Se_3$ precursor's preferred {100} orientation.[248]

2. Emitter Structures

The earliest diode structure reported in CIS was a homojunction device that used the amphoteric nature of CIS to form a junction by annealing a *p*–type $CuInSe_2$ single-crystal in indium to convert its surface to *n*–type CIS.[20] This approach is generally undesirable for photodiodes given the high absorption coefficient of $CuInSe_2$ and relatively poor hole transport in *n*–type CIS, yielding low voltage and photocurrent. Subsequent research investigated the diffusion of the extrinsic dopants cadmium and zinc from Group II of the periodic table to form photodiodes,[85] which did not resolve the problems with the prior approach. The next breakthrough in performance came from the fabrication of *n*–CdS/*p*–$CuInSe_2$ heteroface diodes,[212] which shifts most of the absorption and generation into the *p*–type $CuInSe_2$, because CdS is transparent to photons with energy below its fundamental band-edge at ~ 2.42 eV. Substantial power is still wasted in such a structure because of complete recombination of those carriers generated by photon absorption in the *n*-CdS layer, due to the vanishingly small diffusion length of minority carriers (holes) therein.

Nevertheless, this basic emitter structure was directly applied to thin-film CIS absorber films,[115] with the subsequent addition of an extrinsic indium-dopant to the near-surface part of the CdS emitter to form a n^+–CdS:In layer.[242] Some improvement was later achieved by alloying the CdS with ZnS to increase its bandgap[249] (an improvement previously exploited in copper suldife cells[213]), but the next significant step in the improvement of emitter structures for CIS solar cells was achieved by replacing the extrinsically doped n^+–ZnCdS:In part of the ZnCdS layer, with n^+–ZnO,[250] a higher-bandgap transparent conducting oxide (TCO). This last structure (although usually without zinc in the undoped CdS layer that contacts the CIS) is characteristic of all the highest efficiency devices fabricated nowadays, and the thin (30 to 50 nm) CdS layer is often referred to as the buffer layer. Refinement of the n^+–ZnO/CdS emitter structure to maximize efficiency and yield has led to an additional feature in current high-efficiency implementations, the addition of a high-resistivity ZnO intralayer in the region joining the highly conductive ZnO and the CdS buffer.[251] This is typically achieved either by a change in the ratios of Zn to O reaction precursors to modulate the dopant activation efficiency,[252] or use of different sources[251] without an extrinsic dopant (usually B, In, or Ga) for the high-resistivity portion of the TCO film.

A particularly fascinating and unusual feature of modern CdS buffer layer technology is the sensitive dependence of the device properties on the process used to deposit the buffer. In particular, it has been widely observed that aqueous electroless plating methods, referred to as chemical bath deposition (CBD), yield better devices than any other demonstrated method of CdS deposition.[253] The reasons for this remain an active research area, but there is evidence that this method alters the CI(G)s absorber layer surface[254-257] and

therefore the electronic properties of its interface with the buffer layer.[258-260]

A variety of buffer layer materials other than CdS have been studied as replacements thereof, but none have yet matched its performance.[261] The motivation for replacing CdS is to reduce the cost of safety measures required to protect the environment and workers manufacturing the product, due to the toxicity of the cadmium-containing reactants used for its CBD, as well as the issues of consumer perception and product acceptance. The actual amount of cadmium in a buffer layer a few millionths of a centimeter thick is miniscule and even that is chemically sequestered in the form of CdS, at extremely low net concentrations in a module of < 1 ppm. Alternative buffer layer materials that have been reported include ZnO,[262-266] ZnSe,[267-270] $(Zn,In)_xSe_y$,[271-273] $Zn(O,S,OH)_x$ (or CBD-ZnS),[274-277] $In_x(OH)_y$,[278] $In(OH)_xS_y$,[279-285] and various other less successful materials.

One of the unusual methods of CI(GS)S device optimization commonly used after emitter formation is to bake the cells in oxygen (or simply in air) at a temperature of about 200 to 225°C.[242,286] The influence of oxygen on the electronic properties of polycrystalline CI(GS)S devices has been long recognized and studied.[287,288] This topic has received renewed attention recently because of the interactions between the effects of sodium and those of oxygen and remains a controversial topic.[86,176,289,290] Baking in air to dry the substrates after CBD buffer layer deposition remains a routine part of those processes, and its possible functional equivalence to intentional air annealing should not be ignored.[277,291]

3. Ohmic Contacts

All photodiodes are two-terminal devices, so two ohmic contacts are required, one to the base and the other to the emitter. Although gold or platinum[292] are sometimes used in laboratory research, the base contact to *p*–CIS universally used in application is molybdenum.[293] Molybdenum is susceptible to tarnishing in the high-temperature chalcogenide environments typically encountered during absorber synthesis, which forms the layered compound $Mo(S,Se)_2$ at its interface with CIS,[294,295] or mixtures of these with molybdenum oxides.[296] The extent of this parasitic reaction must be controlled to inhibit the loss of adhesion at the Mo/CIS interface. In addition, because it is a refractory metal, low-temperature deposition processes (e.g., sputtering) can result in very high internal film stress within the molybdenum film itself if proper care is not taken to control this property, which can lead to adhesion loss at the Mo/substrate interface. These potential pitfalls are readily circumvented by modest process optimization and control measures,[297] so molybdenum has been widely adopted as the preferred CI(GS)S electrical contact metallurgy. The use of an alloy (Mo,Cu) contact to improve adhesion has also been demonstrated.[298]

Despite its widespread acceptance for this function, the Mo/*p*–CIS contact may not be purely Ohmic. Studies have shown that there exists a small Schottky barrier between them,[299] which has no effect on the device's I-V characteristics when operated in the PV mode under normal conditions.[300] At low temperatures and in far forward bias, however, the effect of this weak reverse diode can be observed.[301,302]

Another subtle property of the molybdenum contact metallurgy that influences the final PV device performance when it is processed on alkali-glass substrates by high-temperature methods is its permeability to sodium. The complex but profoundly important role of sodium in CIS absorber material optimization has been discussed thoroughly in prior sections of this article. When fabricated on soda-lime glass, the dominant source of sodium is often the substrate,[150,168] which appears to occur primarily by intercalation through its oxidized grain boundaries.[296] This property of the molybdenum films can be very difficult to control, measure, and reproduce, which introduces a large source of variability in the devices' ultimate performance.[151,162] Solutions to this problem remain a very active area of research.

Given the wide variety of emitter structures described in the previous section, it is apparent that a correspondingly wide variety of ohmic contact metallurgies are required. Contacts to the earlier n^+–CdS and n^+–ZnCdS emitter surfaces were usually accomplished with evaporated aluminum grids.[294] The more common n^+–ZnO sur-

face of modern devices can be contacted effectively with a bilayer Ni/Al metalization.[303] The nickel interlayer is used to inhibit the degradation of direct aluminum contacts to ZnO resulting from the oxidation of the aluminum at the interface to form a resistive Al_2O_3 barrier, and consequent loss of ohmic contact.

Another method of contacting the emitter is more common in the monolithically integrated multicell circuits (modules) that can be formed by thin-film processing methods. Although these structures can be made using the contact metallurgies described above,[304] they can also be created by direct contact between the TCO and Mo layers.[305]

4. Superstrate Devices

Most CI(GS)S PV devices are created by first depositing the metallic (usually molybdenum) absorber contact onto a substrate, followed by absorber formation directly onto that contact, and then emitter formation on the free surface of the absorber layer. When made in this sequence, they are called substrate devices and must be illuminated from the side opposite the substrate because of the opaque metallic contact adhered thereto. Alternatively, thin film cells can be built and designed for illumination through the surface on which they are deposited, and are then called superstrate cells.[306] CdTe PV devices are typically made in this manner, as are many amorphous silicon PV devices. For those materials this approach often yields the highest performance, but for the CI(GS)S materials it has not yet worked nearly as well as have substrate devices, with the highest efficiency reported to date of 12.8%.[307]

Superstrate cells may be designed in either a backwall configuration (emitter structure adjacent to the superstrate) or frontwall configuration (absorber between the superstrate and emitter structure), but all the published results in the CIGS material system known to this author are backwall devices.[306,308-310]

B. Fabrication Methods for CIS Absorber Films

Every method of semiconductor processing known to this author has been applied to the synthesis of CIS or its related compounds. Most of these methods have not yielded good device quality materials, or are not suitable for thin-film formation, so only the more successful are detailed in the following subsections. Among these less-developed or applicable methods are the liquid phase bulk crystal growth techniques,[9] direct electrodeposition,[311,312] spray pyrolysis,[262] reactive sputtering,[313,314] flash evaporation,[315] ribbon growth,[316] and metalorganic chemical vapor deposition.[317]

Processes for the formation of CI(GS)S photovoltaic device absorber films universally intend to form the chalcopyrite Cu-III-VI_2 α-phase as their final product. Other phases, both stable and metastable, usually occur during synthesis and appear to be essential to the kinetics of successful methods for device quality absorber film formation. Furthermore, some secondary phases often remain in the completed films as unintended byproducts. Considerable progress has been made in understanding the role of secondary phases in the context of some specific layer synthesis processes.

1. Codeposition

This method was the first high-performance device synthesis method, and the basic method by which all of the record efficiency cells of the last decade have been synthesized. It is characterized by simultaneous exposure of the high-temperature substrate to metal and chalcogenide vapor fluxes. Although these fluxes are most often supplied by multisource elemental evaporation, sputtering of the metals combined with selenium evaporation has been developed[318] to circumvent the target-poisoning problems encountered with reactive sputtering.[319,320]

The role of binary Cu–Se phases during film growth by elemental vacuum co-deposition is probably the best understood of the secondary phase issues alluded to above. This is mostly a consequence of the historical role this process has played in the achievement of record power conversion efficiencies beginning with the demonstration by Chen and Mickelsen of the first >10% CIS cell in 1982[214] and continuing through the current AM 1.5G record of ~19% by the NREL thin

film photovoltaics group.[244] In both cases the deposition of a copper-rich layer during film growth to yield Cu-Se phases was shown to be beneficial to the respective processes, particularly at lower substrate temperatures.[321] Because carrier concentrations in the binary copper selenides are orders of magnitude greater than those of good I-III-VI absorber films, their persistence is deleterious to a device's performance, and their elimination after they have performed their kinetic role in $CuInSe_2$ formation is essential to device optimization.

The earliest 'recipe' for the synthesis of CIS films for high-efficiency photovoltaics (the Boeing bilayer process developed by Mickelsen and Chen[293]) is an *in situ* recrystallization process. In this approach a mixed-phase film layer of $CuInSe_2$ and $Cu_{2-X}Se$ [322] is first deposited at low temperature. This layer then reacts with a copper-deficient flux of coevaporated copper, indium, and selenium vapors at higher temperature to optimize the absorber films's stoichiometry during regrowth on the $CuInSe_2$ nucleation seeds within the initial layer of the films according to the following reaction pathway:

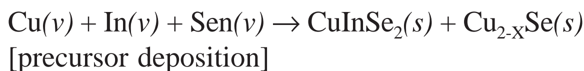

$Cu(v) + In(v) + Sen(v) \rightarrow CuInSe_2(s) + Cu_{2-X}Se(s)$ [precursor deposition]

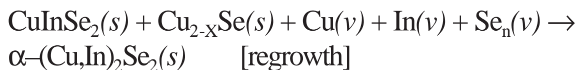

$CuInSe_2(s) + Cu_{2-X}Se(s) + Cu(v) + In(v) + Se_n(v) \rightarrow \alpha\text{–}(Cu,In)_2Se_2(s)$ [regrowth]

This pathway is based on the assumption of near-equilibrium conditions, and to the extent that nonequilibrium components could be involved under some experimental conditions, a more complex description would be required. The partial substitution of gallium for indium in this process leads to greater performance and complexity, with a sensitive dependence on the details of its incorporation.[232]

For a final reaction temperature greater than the 523°C monotectic temperature in the Cu-Se binary system,[178] significantly increased grain size is observed in the final films.[323] This effect is explained as a consequence of melting of $Cu_{2-X}Se$ in the presence of excess selenium, resulting in a liquid phase assisted regrowth process.[324,325] Most evidence indicates that the $Cu_{2-X}Se$ phase is often not completely consumed during this recrystallization process, with small amounts of $Cu_{2-X}Se$ remaining on the $CuInSe_2$ grain boundaries or as inclusions.[295,326]

This approach has been refined continuously and adapted by many researchers,[327] but an apparently different reaction chemistry yielding even higher efficiency devices was reported by Gabor et al.[328] Their three-stage process for growth is based on the reaction chemistry:

$In(v) + Se_n(v) \rightarrow In_2Se_3\,(s)$ [precursor deposition]

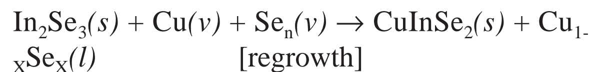

$In_2Se_3(s) + Cu(v) + Se_n(v) \rightarrow CuInSe_2(s) + Cu_{1-X}Se_X(l)$ [regrowth]

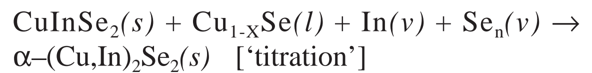

$CuInSe_2(s) + Cu_{1-X}Se(l) + In(v) + Se_n(v) \rightarrow \alpha\text{–}(Cu,In)_2Se_2(s)$ ['titration']

Gallium is substituted in part for indium at each step for CIGS synthesis. A two-stage variant of this process omits the final step but carefully controls the total copper flux in the second stage to minimize the $Cu_{2-X}Se$ phase in the final film.[329] Both of these reaction sequences are in a sense "inverted" processes with respect to the Boeing bilayer recipe.[240] They begin with excess indium as an indium sesquiselenide layer[330] and add copper during the second step. The Boeing bilayer process chemistry begins with excess copper as copper selenide and adds additional indium in the second step.

2. Metal Chalcogenization

This method was first developed by researchers in the mid-1980s, soon after Boeing's development of the coevaporation method. It is characterized by the codeposition of a metal alloy film at relatively low temperatures followed by the conversion of the metal film to a semiconductor film by high-temperature exposure to elemental[245] or, more typically, hydrogenated chalcogenide precursors (e.g., H_2S[331] and/or H_2Se[332]). Precursor metallic layers have been deposited by electrodeposition,[331-333] evaporation,[334] and sputtering.[335] These methods are sometimes referred to as "two-stage" methods.[336]

The reaction chemistries of the metal chalcogenization processes are complex and variable. A large number of intermetallic Cu–In and Cu–Ga alloys can form in these binary systems, and the detailed reaction trajectory of the various implementations of this approach appear to depend sensitively on competing mass transfer and reaction process rates.[231,335]

3. Post-Deposition Thermal Processing

This final category of absorber synthesis methods is more disparate than those preceding it, and overlaps with each of them to some extent. These methods are distinguished by the fact that the component elements of the final absorber compound are all incorporated at relatively low temperature during the deposition stage and are then thermally processed to convert those constituent precursors into the desired structure. In practice these methods often use a chalcogenide vapor overpressure during the second stage to inhibit its loss from the precursor structure, and to that extent are similar to the chalcogenization approach. These methods are also sometimes referred to as "two-stage" methods.[336]

One general category of this type of process is a variation of the metal chalcogenization approach that incorporates elemental selenium directly into a layered precursor structure either as an overlayer,[245] or in a multilayer configuration.[337,338] Heating rate and final anneal temperature have a dramatic effect on the results of this approach, with the best results reported for very high heating rates and final temperatures.[339] The reaction kinetics of this approach appear to be significantly different than that of the hydride-selenization methods.[340,341] A closely related method uses binary selenide precursor layers deposited at low temperatures and then processed at higher temperatures to synthesize the ternary.[342-344] Their similarity lies in the observation that the stacked elemental layer methods yield intermediate binary reaction products very similar to the starting reactants in these binary reaction approaches.[341,343,345]

Another general category of these postdeposition thermal-processing approaches is the particulate-precursor approaches. An early example of this was the screen-printing and sintering of elemental powders.[346] More recent implementations of this approach employ mixed-metal oxide nanoparticle precursors which are reduced and selenized in chalcogen hydride atmospheres,[347] and have achieved efficiencies as high as 12.3%.[348]

C. Opto-Electronic Properties of CIS Devices

The most outstanding properties of CIS photodiodes as opto-electronic devices are notable by virtue of their differences from conventional semiconductor photodiodes. First, the internal quantum efficiency (the ratio of electrons out to photons absorbed) of typical CIS photodiodes measured at zero potential (short-circuit) is almost unity at all wavelengths except those very near the band edge of the absorber or those absorbed in the emitter structure.[293] Such high photocurrents are atypical for PV devices fabricated from conventional semiconductors, and particularly difficult to achieve in their polycrystalline form. On the other hand, the open-circuit voltages of CIS devices are always atypically small fractions of the absorber bandgap energy when compared with PV devices fabricated from conventional semiconductors.[349] Third, stabilization of the steady-state device characteristics of CIS photodiodes subjected to transients in voltage or illumination exhibit some very long time scales compared with PV devices fabricated from conventional semiconductors.[350,351] These first-order differences in device properties are manifestations of the qualitatively different nature of defect chemistry and fundamentally different nature of carrier transport in the ternary copper chalcogenides and their alloys compared with conventional stoichiometric semiconductors,[181] and are still not yet fully understood in detail.

1. Phenomenological Characteristics

In the theory of electronic devices an "ideal diode" is one whose current vs. voltage curve is purely exponential. Real diodes fabricated from

conventional semiconductors can usually be modeled with great accuracy as an equivalent two-terminal circuit containing an ideal diode in both parallel and series with a pair of parasitic resistors. These types of real diodes behave under illumination as if an ideal current source were added in parallel to its diode in that equivalent circuit. Mathematically, the ideal photodiode I-V curves obey a simple principle of translation, with the illuminated and dark curves simply shifted by the short-circuit current.[11]

The ubiquitous nonideality of CIS PV devices is manifested in several characteristic device properties. First, the principle of photocurrent superposition is not obeyed.[352] The illuminated I-V curve of most CIS PV devices is not only shifted by the short-circuit current, but has a different shape. In high-performance devices the difference is subtle, but the deviations from perfect superposition are often obvious and occasionally detrimental to performance (the latter are sometimes referred to as "pathological"). These pathological problems are not necessarily specific to CIS, and similar effects are observed in other thin-film PV device material systems.[229,353,354]

One example of pathological nonideality is the "crossover" effect, where the dark and illuminated I-V curves crossover each other, which cannot occur unless the principle of superposition is violated. Crossover may be caused by photoconductivity in those parts of the device that contribute to parasitic series resistances,[229] by a photo-induced reduction in the junction barrier height,[350] or by a high density of deep electronic defects at the heteroface.[355] A second mode of pathological nonideal photodiode behavior sometimes observed in CIS devices is "rollover" of the illuminated I-V curve in the first quadrant.[356] Modeling and experiments suggest that this may be due to negative charge trapped in deep acceptor states in the junction region that originate from carrier photogeneration in the buffer layer.[357,358]

2. Theory of Operation

When the n-CdS/p- CIS structure was first applied to thin-films of CIS,[115,293] it was assumed that these devices could be characterized electronically as abrupt heterojunction diodes, like those fabricated from conventional semiconductors.[359,360] Subsequent studies using the electron-beam induced current (EBIC) method, however, suggested that the electronic junction was displaced from the metallurgical interface after oxygen baking, repudiating the earlier assumption.[288,361,362] Later research was interpreted to suggest that formation of a copper-deficient n-type ordered defect compound (ODC) between the bulk CIS absorber and the buffer layer was responsible for displacement of the heterojunction from the heteroface.[58] This remains a controversial and very active area of research even today, partly because continuing efforts to replace CdS at the heteroface with some other material have motivated efforts to better understand the reasons that CBD CdS heteroface contacts lead to higher voltage junctions than any other material yet demonstrated. Substitution of cadmium onto vacancies[255,256] left by junction-field-driven electromigration of copper into the bulk,[210,363] has been proposed recently to extrinsically dope and induce type conversion of CI(GS)S, displacing the junction from the heteroface.[364]

The extremely high absorption coefficient of CIS and its alloys of 10^5 cm^{-1} over most of the solar spectrum means that the characteristic depth scale of the absorber's excess carrier pair generation region near the surface is 10^{-5} cm or 100 nm = 0.1 μm. Optimized buffer layers are themselves only slightly thinner than the primary photocarrier generation volume of the device. The exceptionally high excess photocarrier densities generated under typical sunlight exposure near the absorber's surface have long been recognized to result in a number of unusual effects that modify the electric field in the junction region and lead to reduced open-circuit voltage.[365] Theoretical device modeling shows that under solar illumination and biased near the maximum power-point the entire near-junction part of the absorber region is inverted, thereby effectively moving the electronic junction (majority carrier type inversion depth) away from the presumably defective and highly recombinant heteroface.[366]

One cause of nontranslation between dark and light CIS PV device I-V curves is clearly voltage-dependent collection efficiency.[350] This is a

general phenomenon in solar cells, but its effect is negligible in some other types of PV devices.[349] Whereas in the dark all current passing through a photodiode effectively originates at the electrodes, under illumination it is generated non-uniformly throughout the absorber layer. Modulation of the depletion region width with changing bias voltage does not to first-order effect the generation profile, but if the collection probability of minority carriers is substantially different in the space-charge and field-free regions of the absorber, their effective average can vary. Thus, voltage-dependent collection efficiency can yield a violation of the principle of translation between dark and illuminated I-V curves by reducing the current under forward bias below its predicted ideal value. The magnitude of this current reduction in typical CIS devices is estimated to be 2 to 4%.[349]

Another proposed mechanism for the nontranslation between dark and light CIS PV device I-V curves is photo-enhanced tunneling recombination.[352] Recent developments in the analytical modeling of electronic transport in highly doped bipolar semiconductor devices have been applied with remarkable success to the temperature dependence of CIGS PV device I-V curves in the dark.[202] The underlying mechanism of those models is tunneling-enhanced recombination in the space-charge region. These recent developments have not been extended yet to test the earlier photo-enhanced tunneling recombination hypothesis of Miller and Olsen.

To this author's knowledge, no other type of PV device other than those fabricated from the CI(GS)S family of materials share their characteristic of improved performance after extended exposure to light,[350,367,368] although many others degrade after extended exposure. This transient phenomenon is reversible,[363] and characterized by a slow increase in open-circuit and maximum-power voltages with no change in short-circuit current.[351] It has been shown to be a consequence of forward electrical bias itself, rather than illumination per se, and is characterized by time constants of more than 5 min, with full steady-state sometimes taking hours to achieve.[351,363] Some theoretical models propose that this relaxation results from the redistribution of ionized copper atoms in the space-charge region under the influence of the modified internal electric field of the diode when there is photogenerated current.[363,369] The application of spectral methods of electro-optical characterization to the study of these transient processes in CIGS strongly suggest that multiple mechanisms are involved.[370,371] These phenomena remain an active area of current research.[372]

IV. SUMMARY: FUTURE PROSPECTS FOR CIS PHOTOVOLTAICS

It is clear that we still have a great deal to learn about the essential material and structural properties that control the ability of Cu–III–VI_2 devices to convert optical to electrical power. CAIGSS device engineering will benefit from a better understanding of the relationship between junction materials and structure in the critical quarter micron transition region between the emitter and absorber bulk, and the electronic fields, carrier transport, and recombination processes that determine device performance. The experimental difficulty of studying materials properties on this length scale are enormous, and the complexity of the possible chemical defect interactions in these systems, typically containing eight types of atoms, some mobile and ionized acting under the influence of strong electrical field gradients is daunting.

This challenge is balanced by the scientifically intriguing opportunities offered by this material system's unusual status as a chemically disordered crystalline solid that nevertheless shares the tetrahedral adamantine (diamond-like) crystalline structure of silicon. Despite this topological identity of their lattices, photoelectron recombination in *p*–type CIS is relatively unaffected compared with silicon by extended geometric lattice defects like dislocations and grain boundaries. Amorphous silicon provided an earlier historical challenge to the scientific understanding of the relationship between crystallinity and electronic transport in solids, and is another material widely used today to make PV and other electronic devices. The author believes that further investigation of this copper ternary chalcogenide material system offers the scientific community a simi-

lar opportunity to refine its understanding of the relationship between chemical disorder and electronic recombination processes in crystalline solids.

A potentially limiting factor to the large-scale manufacture of CIGSS thin-film PV modules is the availability of the most scarce of its constituent elements, indium. A recent assessment of indium reserves[373] estimated a total worldwide resource of 18,825 metric tons (MT). Unalloyed CIS cells contain about 2 g/μ·m^2 of indium. Current CIGS cell designs with a thickness of 3 μm, 10% overall power conversion efficiency, and 25% gallium substitution for indium would contain about 45MT/GW_p of modules. The overall current indium production rate worldwide is about 285 MT, and the worldwide PV module market for all technologies in 2000 was about 0.12 GW_p. Assuming a continuation of current production rates and a 70% recovery factor, all reserves of indium could be mined out in 66 years, and any increase in demand to satisfy the requirements of a growing CIGS module industry could accelerate this depletion.[373] A reduced absorber thickness and higher module efficiency can be anticipated in more mature technologies to ameliorate the limitations due to this apparent constraint. Finally, there are preliminary indications that previously unrecognized reserves in Asia may significantly increase the true worldwide indium resource.[374]

The intrinsic properties of the CIGSS family of materials clearly make it particularly suitable for thin-film PV device applications. It is both an efficient absorber of light, and its minority carrier recombination properties are uncommonly insensitive to lattice disruptions, including grain boundaries. The latter property relaxes the need for large-grain polycrystalline or single-crystal absorbers. However, the same device design flexibility offered by the ability to tailor these materials' properties by modifying their composition creates a manufacturing challenge due to the need to control that composition. Furthermore, the variability of devices with indistinguishable compositions demonstrates that the crystal defects and structures that control their electronic properties must also be regulated, and these are far more difficult to directly measure than is the overall composition profile. The extent of CIGSS thin-film PV modules' contribution to the world's future energy supplies will depend on our ability to effectively manage this complexity.

ACKNOWLEDGMENTS

The author would like to gratefully acknowledge the contributions of those colleagues who have shared their time and insights with him, thereby considerably influencing the perspectives enunciated herein, although they might not agree with all of this author's conclusions. Among these are David Cahen, Alex Chang, Wen Chen, Albert Davydov, Ingo Dirnstorfer, John Kessler, Hans Neumann, Rommel Noufi, Angus Rockett, Kannan Ramanathan, Bolko von Roedern, Hans Schock, Bill Shafarman, Jim Sites, Lars Stolt, and Su-Huai Wei. This limited specification is not intended to diminish the profound influence of the other authors whose work is cited in the bibliography of this review, but with whom the author has had little opportunity to converse. It has been an honor to join in the progress of our global research community as we have together cast intellectual light onto the mysteries of these still imperfectly understood materials and devices. The financial support of the US Department of Energy and National Renewable Energy Laboratories over many years, most recently'*via* contract XAF 5 14142 10, has enabled this author to participate. The author also thanks Tim Anderson, Bob Birkmire, John Benner, Oscar Crisalle, Tim Coutts, Satyen Deb, Larry Kazmerski, Sheng Li, Tom Surek, Bob Tomlinson, Harin Ullal, and Ken Zweibel for their encouragement.

REFERENCES

1. **Ward, J. S., Ramanathan, K., Hasoon, F. S., Coutts, T. J., Keane, J., Contreras, M. A., Moriarty, T., and Noufi, R.**, *Prog. Photovolt: Res. Appl.*, 10, 41, 2002.
2. **Little, R. G. and Nowlan, M. J.**, *Prog. Photovolt: Res. Appl.*, 5, 309, 1997.
3. **Ullal, H. S., Zweibel, K., and von Roedern, B.**, *Conference Record of the 28th IEEE Photovoltaic Specialists Conference*, IEEE, Piscataway, 301, 2000.

4. **Shay, J. L. and Wernick, J. H.**, *Ternary Chalcopyrite Semiconductors: Growth, Electronic Properties, and Applications*, 1 ed. Permagon Press, Oxford, England, 1975.
5. **Coutts, T. J., Kazmerski, L. L., and Wagner, S.**, *Copper Indium Diselenide for Photovoltaic Applications*, Elsevier Science Ltd., Amsterdam, 1986.
6. **Haneman, D.**, *Crit. Rev. Solid St. Mat. Sci.*, 14, 377, 1988.
7. **Neumann, H. and Tomlinson, R. D.**, *Solar Cells*, 28, 301, 1990.
8. **Rockett, A. and Birkmire, R. W.**, *J. Appl. Phys.*, 70, R81, 1991.
9. **Champness, C. H.**, *J. Mater. Sci.*, 10, 605, 1999.
10. **Rau, U. and Schock, H. W.**, *Appl. Phys. A*, 69, 131, 1999.
11. **Hovel, H. J.**, *Solar Cells*, 1 ed., Academic Press, New York, 1975.
12. **Fonash, S. J.**, *Solar Cell Device Physics*, Academic Press, New York, 1981.
13. **Tsubomura, H. and Kobayashi, H.**, *Crit. Rev. Solid St. Mat. Sci.*, 18, 261, 1993.
14. **Green, M. A.**, *Solar Cells: Operating Principles, Technology, and System Applications*, University of New South Wales, Kensington, 1992.
15. **Partain, L. D.**, Solar Cells and their Applications, John Wiley & Sons, Inc., New York, 1995.
16. **Chopra, K. L. and Das, S. R.**, *Thin Film Solar Cells*, Plenum Press, New York, 1983.
17. **Schock, H. W.**, *Appl. Surf. Sci.*, 92, 606, 1995.
18. **Benner, J. P. and Kazmerski, L.**, Photovoltaics gaining greater visibility, in *IEEE Spectrum*, 36(9), 1999, 34.
19. **Adams, W. G. and Day, R. E.**, *Proc. Royal Soc. A*, 25, 113, 1877.
20. **Parkes, J., Tomlinson, R. D., and Hampshire, M. J.**, *J. Crystal Growth*, 20, 315, 1973.
21. **Rockett, A., Abou-Elfotouh, F., Albin, D., Bode, M., Ermer, J., Klenk, R., Lommasson, T., Russell, T. W. F., Tomlinson, R. D., Tuttle, J., Stolt, L., Walter, T., and Peterson, T. M.**, *Thin Sol. Films*, 237, 1, 1994.
22. **Feigelson, R. S. and Route, R. K.**, *Optical Engineering*, 26, 113, 1987.
23. **Boehnke, U. C. and Kühn, G.**, *J. Mater. Sci.*, 22, 1635, 1987.
24. **Tomlinson, R. D.**, *Ternary and Multinary Compounds, Proceedings of the 7th International Conference*, Deb, S. K. and Zunger, A., Eds., Materials Research Society, Pittsburgh, 177, 1986.
25. **Palatnik, L. S. and Rogacheva, E. I.**, *Sov. Phys. Dokl.*, 12, 503, 1967.
26. **Koneshova, T. I., Babitsyna, A. A., and Kalinnikov, V. T.**, *Izvest. AN SSSR, Neorgan. Mater.*, 18, 1483, 1982.
27. **Fearheiley, M. L.**, *Solar Cells*, 16, 91, 1986.
28. **Folmer, J. C. W., Turner, J. A., Noufi, R., and Cahen, D.**, *J. Electroch. Soc.*, 132, 1319, 1985.
29. **Bachmann, K. J., Fearheily, M. I., Shing, Y. H., and Tran, N.**, *Appl. Phys. Lett.*, 44, 407, 1984.
30. **Bachmann, K. J., Goslowsky, H., and Fiechter, S.**, *J. Crystal Growth*, 89, 160, 1988.
31. **Gödecke, T., Haalboom, T., and Ernst, F.**, *Z. Mettallkd.*, 91, 622, 2000.
32. **Hornung, M.**, Ph.D. thesis University of Freiburg, Shaker–Verlag, Aachen, 1996.
33. **Chang, C. H., Davydov, A., Stanbery, B. J., and Anderson, T. J.**, *The Conference Record of the 25th IEEE Photovoltaic Specialists Conference*, IEEE, Piscataway, 849, 1996.
34. **Haalboom, T., Gödecke, T., Ernst, F., Rühle, M., Herbholz, R., Schock, H. W., Beilharz, C., and Benz, K. W.**, *Ternary and Multinary Compounds, Proceedings of the 11th International Conference*, Inst. Phys. Conf. Ser. 152, Tomlinson, R. D., Hill, A. E., and Pilkington, R. D., Eds., IOP, Bristol, 249, 1997.
35. **Gödecke, T., Haalboom, T., and Ernst, F.**, *Z. Mettallkd.*, 91, 635, 2000.
36. **Gödecke, T., Haalboom, T., and Ernst, F.**, *Z. Mettallkd.*, 91, 651, 2000.
37. **Stanbery, B. J.**, Heteroepitaxy and Nucleation Control for the Growth of Metal Chalcogenides using Activated Reactant Sources, Ph.D. Dissertation, University of Florida, 2001.
38. **Tomm, Y., Fiechter, S., and Fischer, C.**, *Ternary and Multinary Compounds, Proceedings of the 11th International Conference*, Inst. Phys. Conf. Ser. 152, Tomlinson, R. D., Hill, A. E., and Pilkington, R. D., Eds., IOP, Bristol, 181, 1997.
39. **Palatnik, L. S. and Belova, I. K.**, *Izvest. AN SSSR, Neorgan. Mater.*, 12, 2194, 1967.
40. **Mikkelsen, J. C., Jr.**, *J. Electr. Mater.*, 10, 541, 1981.
41. **Binsma, J. J. M., Giling, L. J., and Bloem, J.**, *J. Crystal Growth*, 50, 429, 1980.
42. **Verheijen, A. W., Giling, L. J., and Bloem, J.**, *Mater. Res. Bull.*, 14, 237, 1979.
43. **Migge, H. and Grzanna, J.**, *J. Mater. Res.*, 9, 125, 1994.
44. **Abasova, A. Z., Gasanova, L. G., and Kyazymzade, A. G.**, *Ternary and Multinary Compounds, Proceedings of the 11th International Conference*, Inst. Phys. Conf. Ser. 152, Tomlinson, R. D., Hill, A. E., and Pilkington, R. D., Eds., IOP, Bristol, 87, 1997.
45. **Fiechter, S., Diesner, K., and Tomm, Y.**, *Ternary and Multinary Compounds, Proceedings of the 11th International Conference*, Inst. Phys. Conf. Ser. 152, Tomlinson, R. D., Hill, A. E., and Pilkington, R. D., Eds., IOP, Bristol, 27, 1997.
46. **Grimm, H. G. and Sommerfield, A.**, *Z. Phys.*, 36, 439, 1926.
47. **Zunger, A. and Jaffe, J. E.**, *Phys. Rev. Lett.*, 51, 662, 1983.
48. **Spiess, H. W., Haeberlen, U., Brandt, G., Räuber, A., and Schneider, J.**, *Phys. Stat. Sol. (b)*, 62, 183, 1974.

49. **Chang, C. H., Wei, S. H., Johnson, J. W., Battacharya, R. N., Stanbery, B. J., Anderson, T. J., and Duran, R.**, *Jpn. J. Appl. Phys.*, Suppl. 39-1, 411, 2000.
50. **Chang, C.-H.**, Processing and Characterization of Copper Indium Selenide for Photovoltaic Applications, Ph.D. Dissertation, University of Florida, 1999.
51. **Wei, S.-H., Ferreira, L. G., and Zunger, A.**, *Phys. Rev. B*, 45, 2533, 1992.
52. **Swalin, R. A.**, *Thermodynamics of Solids*, 2nd ed. John Wiley & Sons, New York, 1972.
53. **Chang, C.-H., Wei, S.-H., Ahrenkiel, S. P., Johnson, J. W., Stanbery, B. J., Anderson, T. J., Zhang, S. B., Al-Jassim, M. M., Bunker, G., Payzant, E. A., and Duran, R.**, *II–VI Compound Semiconductor Photovoltaic Materials*, MRS Symposium Proceedings 668, Birkmire, R. et al., Eds., MRS, Warrendale, H4.3.1, 2001.
54. **Delgado, J. M.**, *Ternary and Multinary Compounds, Proceedings of the 11th International Conference*, Inst. Phys. Conf. Ser. 152, Tomlinson, R. D., Hill, A. E., and Pilkington, R. D., Eds., IOP, Bristol, 45, 1997.
55. **Leicht, M., Stenkamp, D., Strunk, H. P., Hornung, M., Beilharz, C., and Benz, K. W.**, *Ternary and Multinary Compounds, Proceedings of the 11th International Conference*, Inst. Phys. Conf. Ser. 152, Tomlinson, R. D., Hill, A. E., and Pilkington, R. D., Eds., IOP, Bristol, 31, 1997.
56. **Leicht, M., Stenkamp, D., and Strunk, H. P.**, *Philos. Mag. A*, 79, 1033, 1999.
57. **Hönle, W., Kühn, G., and Boehnke, U.-C.**, *Crys. Res. Tech.*, 23, 1347, 1988.
58. **Schmid, D., Ruckh, M., Grunwald, F., and Schock, H. W.**, *J. Appl. Phys.*, 73, 2902, 1993.
59. **Scheer, R. and Lewerenz, H.-J.**, *J. Vac. Sci. Tech. A*, 13, 1924, 1995.
60. **Schmid, D., Ruckh, M., and Schock, H. W.**, *Appl. Surf. Sci.*, 103, 409, 1996.
61. **Herberholz, R., Schock, H. W., Rau, U., Werner, J. H., Haalboom, T., Godecke, T., Ernst, F., Beilharz, C., Benz, K. W., and Cahen, D.**, *Conference Record of the 26th IEEE Photovoltaic Specialists Conference*, IEEE, Piscataway, 323, 1997.
62. **Ashcroft, N. W. and Mermin, N. D.**, *Solid State Physics*, 1st ed. Holt, Rinehart and Winston, New York, 1976.
63. **Gödecke, T., Haalboom, T., and Sommer, F.**, *J. Phase Equil.*, 19, 576, 1998.
64. **Collongues, R.**, *Jap. J. Appl. Phys.*, 32–3, 442, 1993.
65. **Bode, M. H.**, *J. Appl. Phys.*, 76, 159, 1994.
66. **Kuan, T. S., Kuech, T. F., Wang, W. I., and Wilkie, E. L.**, *Phys. Rev. Lett.*, 54, 201, 1985.
67. **Su, D. S., Neumann, W., Hunger, R., Schubert-Bischoff, P., Giersig, M., Lewerenz, H. J., Scheer, R., and Zeitler, E.**, *Appl. Phys. Lett.*, 73, 785, 1998.
68. **Fons, P., Niki, S., Yamanda, A., and Oyanagi, H.**, *J. Appl. Phys.*, 84, 6926, 1998.
69. **Panchekha, P., Boyko, B., Novikov, V., and Chernikov, A.**, *Proceedings of the 2nd World Conference on Photovoltaic Solar Energy Conversion*, EC Joint Research Centre, Brussels, 485, 1998.
70. **Horikoshi, Y., Kawashima, M., and Yamaguchi, H.**, *Jpn. J. Appl. Phys.*, 25, L868, 1986.
71. **Stanbery, B. J., Chang, C. H., Kim, S., Kincal, S., Lippold, G., Ahrenkiel, S. P., Li, L., Anderson, T. J., and Al-Jassim, M. M.**, *Self-Organized Processes in Semiconductor Alloys*, MRS Symposium Proceedings 583, Mascarenhas, A. et al., Eds., MRS, Warrendale, 195, 1999.
72. **Stanbery, B. J., Kincal, S., Kim, S., Chang, C. H., Ahrenkiel, S. P., Lippold, G., Neumann, H., Anderson, T. J., and Crisalle, O. D.**, *J. Appl. Phys.*, 91, 3598, 2002.
73. **Wei, S.-H., Zhang, S. B., and Zunger, A.**, *Phys. Rev. B*, 59, R2478, 1999.
74. **Groenink, A. and Janse, P. H.**, *Z. Physik. Chem. Neue Folge*, 110, 17, 1978.
75. **Schmalzried, H.**, *Progr. Solid State Chem.*, 2, 265, 1965.
76. **Rincón, C. and Wasim, S. M.**, *Ternary and Multinary Compounds, Proceedings of the 7th International Conference*, Deb, S. K. and Zunger, A., Eds., MRS, Pittsburgh, 443, 1986.
77. **Endo, S., Irie, T., and Nakanishi, H.**, *Solar Cells*, 16, 1, 1986.
78. **Rincón, C. and Bellabarba, C.**, *Phys. Rev. B*, 33, 7160, 1986.
79. **Wasim, S. M.**, *Solar Cells*, 16, 289, 1986.
80. **Flygare, W. H.**, *Molecular Structure and Dynamics*, 1st ed. Prentice–Hall, Englewood Cliffs, 1978.
81. **Zhang, S. B., Wei, S.-H., Zunger, A., and Katayama-Yoshida, H.**, *Phys. Rev. B*, 57, 9642, 1998.
82. **Zhang, S. B., Wei, S.-H., and Zunger, A.**, *Phys. Rev. Lett.*, 78, 4059, 1997.
83. **Rockett, A.**, *Thin Sol. Films*, 361-362, 330, 2000.
84. **Parthé, E.**, *Elements of Inorganic Structural Chemistry*, 2nd ed. Sutter-Parthé, Petit-Lancy, Switzerland, 1996.
85. **Migliorato, P., Shay, J. L., Kasper, H. M., and Wagner, S.**, *J. Appl. Phys.*, 46, 1777, 1975.
86. **Wei, S.-H., Zhang, S. B., and Zunger, A.**, *J. Appl. Phys.*, 85, 7214, 1999.
87. **Suzuki, R., Ohdaira, T., Ishibashi, S., Uedono, A., Niki, S., Fons, P. J., Yamada, A., Mikado, T., Yamazaki, T., and Tanigawa, S.**, *Ternary and Multinary Compounds, Proceedings of the 11th International Conference*, Inst. Phys. Conf. Ser. 152, Tomlinson, R. D., Hill, A. E., and Pilkington, R. D., Eds., IOP, Bristol, 757, 1997.
88. **Niki, S., Suzuki, R., Ishibashi, S., Ohdaira, T., Fons, P. J., Yamada, A., and Oyanagi, H.**, *Proceedings of the 2nd World Conference on Photovoltaic Solar Energy Conversion*, EC Joint Research Centre, Brussels, 616, 1998.

89. **Suzuki, R., Ohdaira, T., Ishibashi, S., Niki, S., Fons, P. J., Yamada, A., Mikado, T., Yamazaki, T., Uedono, A., and Tanigawa, S.**, *Proceedings of the 2nd World Conference on Photovoltaic Solar Energy Conversion*, EC Joint Research Centre, Brussels, 620, 1998.
90. **Van Vechten, J. A.**, *Ternary and Multinary Compounds, Proceedings of the 7th International Conference*, Deb, S. K. and Zunger, A., Eds., Materials Research Society, Pittsburgh, 423, 1986.
91. **Pankove, J. I.**, *Optical Processes in Semiconductors*, Dover Publications, Inc., New York, 1971.
92. **Urbach, F.**, *Phys. Rev.*, 92, 1324, 1953.
93. **Redfield, D.**, *Phys. Rev.*, 130, 916, 1963.
94. **Redfield, D. and Afromowitz, M. A.**, *Appl. Phys. Lett.*, 11, 138, 1967.
95. **Mahan, G. D. and Conley, J. W.**, *Appl. Phys. Lett.*, 11, 29, 1967.
96. **Nakanishi, H., Sawaya, T., Endo, S., and Irie, T.**, *Jpn. J. Appl. Phys.*, 32–3, 200, 1993.
97. **Dow, J. D. and Redfield, D.**, *Phys. Rev. B*, 5, 594, 1972.
98. **Kurkik, M. V.**, *Phys. Stat. Sol. (a)*, 8, 9, 1971.
99. **Medvedkin, G. A. and Magomedov, M. A.**, *J. Appl. Phys.*, 82, 4013, 1997.
100. **Ikari, T., Yoshino, K., Shimizu, T., Fukuyama, A., Maeda, K., Fons, P. J., Yamada, A., and Niki, S.**, *Ternary and Multinary Compounds, Proceedings of the 11th International Conference*, Inst. Phys. Conf. Ser. 152, Tomlinson, R. D., Hill, A. E., and Pilkington, R. D., Eds., IOP, Bristol, 511, 1997.
101. **Hahn, T.**, International Tables for Crystallography: Space-Group Symmetry, Kluwer Academic Publishers, Dordrecht, A, 1996.
102. **Tanino, H., Maeda, T., Fujikake, H., Nakanishi, H., Endo, S., and Irie, T.**, *Phys. Rev. B*, 45, 13323, 1992.
103. **Rincón, C. and Ramirez, F. J.**, *J. Appl. Phys.*, 72, 4321, 1992.
104. **Wakita, K., Hirooka, H., Yasuda, S., Fujita, F., and Yamamoto, N.**, *J. Appl. Phys.*, 83, 443, 1998.
105. **Yamamoto, N., Susaki, M., and Wakita, K.**, *J. Lumin.*, 87–89, 226, 2000.
106. **Yamamoto, N., Susaki, M., Huang, W.-Z., and Wakita, K.**, *Crys. Res. Tech.*, 31, S369, 1996.
107. **Nomura, S., O'Uchi, S., and Endo, S.**, *Ternary and Multinary Compounds, Proceedings of the 11th International Conference*, Inst. Phys. Conf. Ser. 152, Tomlinson, R. D., Hill, A. E., and Pilkington, R. D., Eds., IOP, Bristol, 649, 1997.
108. **Rincón, C., Wasim, S. M., Marin, G., Delgado, J. M., Huntzinger, J. R., Zwick, A., and Galibert, J.**, *Appl. Phys. Lett.*, 73, 441, 1998.
109. **Rincón, C., Wasim, S. M., Marin, G., Hernandez, E., Perez, G. S., and Galibert, J.**, *J. Appl. Phys.*, 87, 2293, 2000.
110. **Nelson, A. J., Horner, G. S., Sinha, K., and Bode, M. H.**, *Appl. Phys. Lett.*, 64, 3600, 1994.
111. **Parkes, J., Tomlinson, R. D., and Hampshire, M. J.**, *Solid State Electron.*, 16, 773, 1973.
112. **Shay, J. L., Tell, B., Kasper, H. M., and Schiavone, L. M.**, *Phys. Rev. B*, 7, 4485, 1973.
113. **Hörig, W., Neumann, H., and Sobotta, H.**, *Thin Sol. Films*, 48, 67, 1978.
114. **Rincón, C. and González, J.**, *Phys. Stat. Sol. (b)*, 118, K21, 1983.
115. **Kazmerski, L. L., White, F. R., and Morgan, G. K.**, *Appl. Phys. Lett.*, 29, 268, 1976.
116. **Nakanishi, H., Endo, S., Irie, T., and Chang, B. H.**, *Ternary and Multinary Compounds, Proceedings of the 7th International Conference*, Deb, S. K. and Zunger, A., Eds., Materials Research Society, Pittsburgh, 99, 1986.
117. **Niki, S., Shibata, H., Fons, P. J., Yamada, A., Obara, A., Makita, Y., Kurafuji, T., Chichibu, S., and Nakanishi, H.**, *Appl. Phys. Lett.*, 67, 1289, 1995.
118. **Varshni, Y. P.**, *Physica*, 34, 149, 1967.
119. **Yu, P. W.**, *J. Appl. Phys.*, 47, 677, 1976.
120. **Lárez, C., Bellabarba, C., and Rincon, C.**, *Appl. Phys. Lett.*, 65, 1650, 1994.
121. **Manoogian, A. and Woolley, J. C.**, *Can. J. Phys.*, 62, 285, 1983.
122. **Rincón, C.**, *Phys. Stat. Sol. (a)*, 134, 383, 1992.
123. **Abou-Elfotouh, F. A., Moutinho, H., Bakry, A., Coutts, T. J., and Kazmerski, L. L.**, *Solar Cells*, 30, 151, 1991.
124. **Bottomley, D. J., Mito, A., Niki, S., and Yamada, A.**, *Appl. Phys. Lett.*, 82, 817, 1997.
125. **Xiao, H. Z., Yang, L.-C., and Rockett, A.**, *J. Appl. Phys.*, 76, 1503, 1994.
126. **Wasim, S. M., Marin, G., Rincón, C., Bocaranda, P., Mazón, C., Pérez, S. G., Mora, A. E., Iqbal, M., and Bacquet, G.**, *Ternary and Multinary Compounds, Proceedings of the 11th International Conference*, Inst. Phys. Conf. Ser. 152, Tomlinson, R. D., Hill, A. E., and Pilkington, R. D., Eds., IOP, Bristol, 55, 1997.
127. **Boyd, G. D., Kasper, H. M., McFee, J. H., and Storz, F. G.**, *IEEE J. Quantum Electr.*, QE8, 900, 1972.
128. **Angelov, M., Goldhahn, R., Gobsch, G., Kanis, M., and Fiechter, S.**, *J. Appl. Phys.*, 75, 5361, 1994.
129. **Hsu, T. M., Chang, H. Y., Hwang, H. L., and Lee, S. Y.**, *Ternary and Multinary Compounds, Proceedings of the 7th International Conference*, Deb, S. K. and Zunger, A., Eds., Materials Research Society, Pittsburgh, 93, 1986.
130. **Hsu, T. M.**, *J. Appl. Phys.*, 59, 2538, 1986.
131. **Binsma, J. J. M., Giling, L. J., and Bloem, J.**, *J. Lumin.*, 27, 55, 1982.
132. **Hsu, T. M., Lee, J. S., and Hwang, H. L.**, *J. Appl. Phys.*, 68, 283, 1990.
133. **Boyd, G. D., Kasper, H. M., and McFee, J. H.**, *IEEE J. Quantum Electr.*, QE7, 563, 1971.
134. **Gabor, A. M., Tuttle, J. R., Schwartzlander, A., Tennant, A. L., Contreras, M. A., and Noufi, R.**,

Proceedings of the 1st World Conference on Photovoltaic Energy Conversion, IEEE, Piscataway, 83, 1994.
135. **Beilharz, C.**, *Charakterisierung von aus der Schmelze gezüchteten Kristallen in den Systemen Kupfer–Indium–Selen und Kupfer-Indium–Gallium–Selen für photovoltaische Anwendungen*, Shaker Verlag, Aachen, 1999.
136. **Shafarman, W. N., Klenk, R., and McCandless, B. E.**, *J. Appl. Phys.*, 79, 7324, 1996.
137. **Herberholz, R., Nadenau, V., Ruhle, U., Koble, C., Schock, H. W., and Dimmler, B.**, *Solar Energy Mat. Sol. Cells*, 49, 227, 1997.
138. **Wei, S.-H., Zhang, S. B., and Zunger, A.**, *Appl. Phys. Lett.*, 72, 3199, 1998.
139. **Schroeder, D. J., Hernandez, J. L., Berry, G. D., and Rockett, A. A.**, *J. Appl. Phys.*, 83, 1519, 1998.
140. **Chen, A.-B. and Sher, A.**, *Semiconductor Alloys: Physics and Materials Engineering*, Plenum Press, New York, 1995.
141. **Albin, D. S., Tuttle, J. R., Mooney, G. D., Carapella, J. J., Duda, A., Mason, A., and Noufi, R.**, *The Conference Record of the 21st IEEE Photovoltaic Specialists Conference*, IEEE, New York, 562, 1990.
142. **Chen, W. S., Stewart, J. M., Stanbery, B. J., Devany, W. E., and Mickelsen, R. A.**, *The Conference Record of the 19th IEEE Photovoltaic Specialists Conference*, IEEE, New York, 1445, 1987.
143. **Ciszek, T. F., Bacewicz, R., Durrant, J. R., Deb, S. K., and Dunlavy, D.**, *The Conference Record of the 19th IEEE Photovoltaic Specialists Conference*, IEEE, New York, 1448, 1987.
144. **Bodnar, I. V., Bologa, A. P., and Korzun, B. V.**, *Phys. Stat. Sol. (b)*, 109, K31, 1982.
145. **Bodnar, I. V., Korzun, B. V., and Lakomskii, A. J.**, *Phys. Stat. Sol. (b)*, 105, K143, 1981.
146. **Neff, H., Lange, P., Fearheiley, M. L., and Bachmann, K. J.**, *Appl. Phys. Lett.*, 47, 1089, 1985.
147. **Miyake, H., Tsuda, M., and Sugiyama, K.**, *Ternary and Multinary Compounds, Proceedings of the 11th International Conference*, Inst. Phys. Conf. Ser. 152, Tomlinson, R. D., Hill, A. E., and Pilkington, R. D., Eds., IOP, Bristol, 83, 1997.
148. **Shirakata, S., Ogawa, A., Isomura, S., and Kariya, T.**, *Jap. J. Appl. Phys.*, 32 Supplement 32–3, 94, 1993.
149. **Antonioli, G., Bini, S., Lottici, P. P., Razzetti, C., and Vlaic, G.**, *Ternary and Multinary Compounds, Proceedings of the 7th International Conference*, Deb, S. K. and Zunger, A., Eds., Materials Research Society, Pittsburgh, 149, 1986.
150. **Hedström, J., Ohlsén, H., Bodegård, M., Kylner, A., Stolt, L., Hariskos, D., Ruckh, M., and Schock, H.-W.**, *The Conference Record of the 23rd IEEE Photovoltaic Specialists Conference*, IEEE, Piscataway, 364, 1993.
151. **Rockett, A., Granath, K., Asher, S., Jassim, M. M. A., Hasoon, F., Matson, R., Basol, B., Kapur, V., Britt, J. S., Gillespie, T., and Marshall, C.**, *Solar Energy Mat. and Sol. Cells*, 59, 255, 1999.
152. **Probst, V., Rimmasch, J., Riedl, W., Stetter, W., Holz, J., Harms, H., Karg, F., and Schock, H. W.**, *Proceedings of the 1st World Conference on Photovoltaic Energy Conversion*, IEEE, Piscataway, 144, 1994.
153. **Bodegård, M., Hedström, J., Granath, K., Rockett, A., and Stolt, L.**, *Proceedings of the 13th European Photovoltaic Solar Energy Conference*, H.S. Stephens & Associates, Bedford, 2080, 1995.
154. **Granath, K., Bodegård, M., and Stolt, L.**, *Solar Energy Mat. and Sol. Cells*, 60, 279, 1999.
155. **Rau, U., Schmitt, M., Hilburger, D., Engelhardt, F., Seifert, O., and Parisi, J.**, *The Conference Record of the 25th IEEE Photovoltaic Specialists Conference*, IEEE, Piscataway, 1005, 1996.
156. **Granata, J. E., Sites, J. R., Asher, S., and Matson, R. J.**, *Conference Record of the 26th IEEE Photovoltaic Specialists Conference*, IEEE, Piscataway, 387, 1997.
157. **Granata, J. E. and Sites, J. R.**, *Proceedings of the* 2nd *World Conference on Photovoltaic Solar Energy Conversion*, EC Joint Research Centre, Brussels, 604, 1998.
158. **Rau, U., Schmitt, M., Engelhardt, F., Seifert, O., Parisi, J., Riedl, W., Rimmasch, J., and Karg, F.**, *Solid State Comm.*, 107, 59, 1998.
159. **Niles, D. W., Ramanathan, K., Hasoon, F., Noufi, R., Tielsch, B. J., and Fulghum, J. E.**, *J. Vac. Sci. Tech. A*, 15, 3044, 1997.
160. **Rockett, A., Bodegård, M., Granath, K., and Stolt, L.**, *The Conference Record of the 25th IEEE Photovoltaic Specialists Conference*, IEEE, Piscataway, 985, 1996.
161. **Niles, D. W., Al-Jassim, M., and Ramanathan, K.**, *J. Vac. Sci. Tech. A*, 17, 291, 1999.
162. **Holz, J., Karg, F., and von Philipsborn, H.**, *Proceedings of the 12th European Photovoltaic Solar Energy Conference*, Amsterdam, 1592, 1994.
163. **Keyes, B. M., Hasoon, F., Dippo, P., Balcioglu, A., and Abufotuh, F.**, *Conference Record of the 26th IEEE Photovoltaic Specialists Conference*, IEEE, Piscataway, 479, 1997.
164. **Schroeder, D. J. and Rockett, A. A.**, *J. Appl. Phys.*, 82, 4982, 1997.
165. **Bodegård, M., Stolt, L., and Hedström, J.**, *Proceedings of the 12th European Photovoltaic Solar Energy Conference*, 1743, 1994.
166. **Basol, B. M., Kapur, V. K., Leidholm, C. R., Minnick, A., and Halani, A.**, *The1st World Conference on Photovoltaic Energy Conversion*, IEEE, Piscataway, 147, 1994.
167. **Nakada, T., Ohbo, H., Fukuda, M., and Kunioka, A.**, *Solar Energy Mat. and Sol. Cells*, 49, 261, 1997.
168. **Ruckh, M., Schmid, D., Kaiser, M., Schäffler, R., Walter, T., and Schock, H. W.**, *Proceedings of the*

1st World Conference on Photovoltaic Energy Conversion, IEEE, Piscataway, 156, 1994.

169. **Contreras, M. A., Egaas, B., Dippo, P., Webb, J., Granata, J. E., Ramanathan, K., Asher, S., Swartzlander, A., and Noufi, R.**, *Conference Record of the 26th IEEE Photovoltaic Specialists Conference*, IEEE, Piscataway, 359, 1997.
170. **Stanbery, B. J., Chang, C. H., and Anderson, T. J.**, *Ternary and Multinary Compounds, Proceedings of the 11th International Conference*, Inst. Phys. Conf. Ser. 152, Tomlinson, R. D., Hill, A. E., and Pilkington, R. D., Eds., IOP, Bristol, 915, 1997.
171. **Stanbery, B. J., Davydov, A., Chang, C. H., and Anderson, T. J.**, *NREL/SNL Photovoltaics Program Review, Proceedings of the 14th Conference*, AIP Conference Proceedings 394, Witt, C. E., Al-Jassim, M., and Gee, J. M., Eds., AIP, New York, 579, 1996.
172. **Stanbery, B. J., Lambers, E. S., and Anderson, T. J.**, *Conference Record of the 26th IEEE Photovoltaic Specialists Conference*, IEEE, Piscataway, 499, 1997.
173. **Stanbery, B. J., Kincal, S., Kim, S., Anderson, T. J., Crisalle, O. D., Ahrenkiel, S. P., and Lippold, G.**, *Conference Record of the 28th IEEE Photovoltaic Specialists Conference*, IEEE, Piscataway, 440, 2000.
174. **Klein, A., Loher, T., Pettenkofer, C., and Jaegermann, W.**, *J. Appl. Phys.*, 80, 5039, 1996.
175. **Kronik, L., Cahen, D., and Schock, H. W.**, *Adv. Mater.*, 10, 31, 1998.
176. **Kronik, L., Cahen, D., Rau, U., Herberholz, R., and Schock, H. W.**, *Proceedings of the 2nd World Conference on Photovoltaic Solar Energy Conversion*, EC Joint Research Centre, Brussels, 453, 1998.
177. **Braunger, D., Hariskos, D., Bilger, G., Rau, U., and Schock, H. W.**, *Thin Sol. Films*, 361-362, 161, 2000.
178. **Chakrabarti, D. J. and Laughlin, D. E.**, *Bull. Alloy Phase Diag.*, 2, 305, 1981.
179. **Nomura, S. and Takizawa, T.**, *J. Crystal Growth*, 128, 659, 1993.
180. **Gal'pern, Y. S. and Efros, A. L.**, *Soviet Physics — Semiconductors*, 6, 941, 1972.
181. **Rogacheva, E. I.**, *Ternary and Multinary Compounds, Proceedings of the 11th International Conference*, Inst. Phys. Conf. Ser. 152, Tomlinson, R. D., Hill, A. E., and Pilkington, R. D., Eds., IOP, Bristol, 1, 1997.
182. **Nomura, S., Itoh, J., and Takizawa, T.**, *Jpn. J. Appl. Phys.*, 32 Supplement 32–3, 97, 1993.
183. **Blakemore, J. S.**, *Solid State Physics*, 2nd ed. W. B. Saunders Company, 1974.
184. **Walukiewicz, W.**, *Phys. Rev. B*, 50, 5221, 1994.
185. **Zhang, S. B., Wei, S.-H., and Zunger, A.**, *J. Appl. Phys.*, 83, 3192, 1998.
186. **Shklovskii, B. I. and Efros, A. L.**, *Soviet Physics - Semiconductors*, 4, 249, 1970.
187. **Shklovskii, B. I. and Efros, A. L.**, *Soviet Physics JETP*, 34, 435, 1972.
188. **Efros, A. L. and Shklovskii, B. I.**, *J. Phys. C*, 8, 49, 1975.
189. **Efros, A. L., Lien, N. V., and Shklovskii, B. I.**, *Solid State Comm.*, 32, 851, 1979.
190. **Mott, N. F. and Davis, E. A.**, *Electronic Processes in Non-Crystalline Materials*, Clarendon Press, Oxford, 1971.
191. **Hernández, E., Rincón, C., Wasim, S. M., Marin, G., Bocaranda, P., Bacquet, G., and Peyrade, J. P.**, *Ternary and Multinary Compounds, Proceedings of the 11th International Conference*, Inst. Phys. Conf. Ser. 152, Tomlinson, R. D., Hill, A. E., and Pilkington, R. D., Eds., IOP, Bristol, 915, 1997.
192. **Dirnstorfer, I., Wagner, M., Hofmann, D. M., Lampert, M. D., Karg, F., and Meyer, B. K.**, *Phys. Stat. Sol. (a)*, 168, 163, 1998.
193. **Zott, S., Leo, K., Ruckh, M., and Schock, H.-W.**, *The Conference Record of the 25th IEEE Photovoltaic Specialists Conference*, IEEE, Piscataway, 817, 1996.
194. **Zott, S., Leo, K., Ruckh, M., and Schock, H.-W.**, *J. Appl. Phys.*, 82, 356, 1997.
195. **Thomas, D. G., Hopfield, J. J., and Augustyniak, W. M.**, *Phys. Rev. A*, 140, 202, 1965.
196. **Shklovskii, B. I. and Efros, A. L.**, *Electronic Properties of Doped Semiconductors*, Springer-Verlag, New York, 1984.
197. **Shklovskii, B. I., Shur, M. S., and Efros, A. L.**, *Soviet Physics — Semiconductors*, 5, 1682, 1972.
198. **Ziman, J. M.**, *Models of Disorder: the Theoretical Physics of Homogeneously Disordered Systems*, Cambridge University Press, Oxford, 1979.
199. **Shirakata, S., Chichibu, S., Miyake, H., Isomura, S., Nakanishi, H., and Sugiyama, K.**, *Ternary and Multinary Compounds, Proceedings of the 11th International Conference*, Inst. Phys. Conf. Ser. 152, Tomlinson, R. D., Hill, A. E., and Pilkington, R. D., Eds., Institute of Physics, Bristol, 597, 1997.
200. **Hall, R. N.**, *Phys. Rev.*, 87, 387, 1952.
201. **Shockley, W. and Read, W.**, *Phys. Rev.*, 87, 835, 1952.
202. **Rau, U.**, *Appl. Phys. Lett.*, 74, 111, 1999.
203. **von Roedern, B.**, *Applied Physics Communications*, 12, 45, 1993.
204. **von Roedern, B. and Bauer, G. H.**, *Amorphous and Heterogeneous Silicon Thin Films: Fundamentals to Devices*, Mat. Res. Soc. Symp. Proc. 577, Branz, H. M. et al., Eds., MRS, Warrendale, 761, 1999.
205. **Boyce, J. B., Hayes, T. M., and Mikkelsen, J., J. C.**, *Solid State Ion.*, 5, 497, 1981.
206. **Dagan, G., Ciszek, T. F., and Cahen, D.**, *J. Phys. Chem.*, 96, 11009, 1992.
207. **Chernyak, L., Stafsudd, O., and Cahen, D.**, *J. Phys. Chem. Sol.*, 56, 1165, 1995.
208. **Gartsman, K., Chernyak, L., Lyahovitskaya, V., Cahen, D., Didik, V., Kozlovsky, V., Malkovich, R., Skoryatine, E., and Usacheva, V.**, *J. Appl. Phys.*, 82, 4282, 1997.
209. **Nadazdy, V., Yakushev, M., Kjebbar, E. H., Hill, A. E., and Tomlinson, R. D.**, *J. Appl. Phys.*, 84, 4322, 1998.

210. **Klein, A. and Jaegermann, W.**, *Appl. Phys. Lett.*, 74, 2283, 1999.
211. **Hermann, A. M. and Fabick, L.**, *J. Crystal Growth*, 61, 658, 1983.
212. **Shay, J. L., Wagner, S., and Kasper, H. M.**, *Appl. Phys. Lett.*, 27, 89, 1975.
213. **Hall, R. B., Birkmire, R. W., Phillips, J. E., and Meakin, J. D.**, *The Conference Record of the 15th IEEE Photovoltaic Specialists Conference*, IEEE, New York, 777, 1981.
214. **Mickelsen, R. A. and Chen, W. S.**, *The Conference Record of the 16th IEEE Photovoltaic Specialists Conference*, IEEE, New York, 781, 1982.
215. **Catalano, A., D'Aiello, R. V., Dresner, J., Faughnan, B., Firester, A., Kane, J., Schade, H., Smith, Z. E., Swartz, G., and Triano, A.**, *The Conference Record of the 16th IEEE Photovoltaic Specialists Conference*, IEEE, New York, 1421, 1982.
216. **Loferski, J. J.**, *J. Appl. Phys.*, 27, 777, 1956.
217. **Shockley, W. and Queisser, H. J.**, *J. Appl. Phys.*, 32, 510, 1961.
218. **Mathers, C. D.**, *J. Appl. Phys.*, 48, 3181, 1977.
219. **Kukimoto, H.**, *Jap. J. Appl. Phys.*, 32–3, 10, 1993.
220. **Itoh, F., Saitoh, O., Kita, M., Nagamore, H., and Oike, H.**, *Solar Energy Mat. and Sol. Cells*, 50, 119, 1996.
221. **Haimbodi, M. W., Gourmelon, E., Paulson, P. D., Birkmire, R. W., and Shafarman, W. N.**, *Conference Record of the 28th IEEE Photovoltaic Specialists Conference*, IEEE, Piscataway, 454, 2000.
222. **Walter, T., Content, A., Velthaus, K. O., and Schock, H. W.**, *Solar Energy Mat. and Sol. Cells*, 26, 357, 1992.
223. **Fan, J. C. C., Tsaur, B. Y., and Palm, B. J.**, *The Conference Record of the 16th IEEE Photovoltaic Specialists Conference*, IEEE, New York, 692, 1982.
224. **Bellabarba, C. and Rincon, C.**, *Jpn. J. Appl. Phys.*, 32–3, 599, 1993.
225. **Barnett, A. M. and Rothwarf, A.**, *IEEE Trans. Elec. Dev.*, ED-27, 615, 1980.
226. **Pauwels, H. J., De Visschere, P., and Reussens, P.**, *Solid State Electron.*, 21, 775, 1978.
227. **Liu, X. X. and Sites, J. R.**, *The Conference Record of the 23rd IEEE Photovoltaic Specialists Conference*, IEEE, Piscataway, 501, 1993.
228. **Weigand, R., Bacher, G., Ohnesorge, B., Forchel, A., Riedl, W., and Karg, F. H.**, *Proceedings of the 2nd World Conference on Photovoltaic Solar Energy Conversion*, EC Joint Research Centre, Brussels, 573, 1998.
229. **Rothwarf, A. and Boer, K. W.**, *Progr. Solid State Chem.*, 10, 71, 1975.
230. **Walter, T. and Schock, H. W.**, *Thin Sol. Films*, 224, 74, 1993.
231. **Marudachalam, M., Birkmire, R. W., Hichri, H., Schultz, J. M., Swartzlander, A., and Al-Jassim, M. M.**, *J. Appl. Phys.*, 82, 2896, 1997.
232. **Bodegård, M., Kessler, J., Lundberg, O., Schöldström, J., and Stolt, L.**, *II–VI Compound Semiconductor Photovoltaic Materials*, MRS Symposium Proceedings 668, Birkmire, R. et al., Eds., MRS, Warrendale, H2.2.1, 2001.
233. **Marudachalam, M., Hichri, H., Birkmire, R. W., and Schultz, J. M.**, *Appl. Phys. Lett.*, 67, 3978, 1995.
234. **Contreras, M., Tuttle, J., Du, D., Qi, Y., Swartzlander, A., Tennant, A., and Noufi, R.**, *Appl. Phys. Lett.*, 63, 1824, 1993.
235. **Shafarman, W. N., Klenk, R., and McCandless, B. E.**, *The Conference Record of the 25th IEEE Photovoltaic Specialists Conference*, IEEE, Piscataway, 763, 1996.
236. **Bodegård, M., Lundberg, O., Malmström, J., and Stolt, L.**, *Conference Record of the 28th IEEE Photovoltaic Specialists Conference*, IEEE, Piscataway, 450, 2000.
237. **Schwartz, R. J. and Gray, J. L.**, *The Conference Record of the 21st IEEE Photovoltaic Specialists Conference* 1, IEEE, New York, 570, 1990.
238. **von Roedern, B.**, *Proceedings of the 12th European Photovoltaic Solar Energy Conference*, Amsterdam, 1354, 1994.
239. **Tarrant, D. and Ermer, J.**, *The Conference Record of the 23rd IEEE Photovoltaic Specialists Conference*, IEEE, Piscataway, 372, 1993.
240. **Zweigart, S., Walter, T., Köble, C., Sun, S. M., Rühle, U., and Schock, H. W.**, *Proceedings of the 1st World Conference on Photovoltaic Energy Conversion*, IEEE, Piscataway, 60, 1994.
241. **Noufi, R., Axton, R., Cahen, D., and Deb, S. K.**, *The Conference Record of the 17th IEEE Photovoltaic Specialists Conference*, IEEE, New York, 927, 1984.
242. **Mickelsen, R. A. and Chen, W. S.**, *The Conference Record of the 15th IEEE Photovoltaic Specialists Conference*, IEEE, Piscataway, 800, 1981.
243. **Gabor, A. M., Tuttle, J. R., Albin, D. S., Tennant, A. L., Contreras, M. A., and Noufi, R.**, *12th NREL Photovoltaics Program Review*, AIP Conference Series 306, AIP, Woodbury, 59, 1993.
244. **Contreras, M. A., Egaas, B., Ramanathan, K., Hiltner, J., Swartzlander, A., Hasoon, F., and Noufi, R.**, *Prog. Photovolt: Res. Appl.*, 7, 311, 1999.
245. **Dimmler, B., Dittrich, H., and Schock, H. W.**, *The Conference Record of the 20th IEEE Photovoltaic Specialists Conference* 2, IEEE, New York, 1426, 1988.
246. **Kiely, C. J., Pond, R. C., Kenshole, G., and Rockett, A.**, *Philos. Mag. A*, 63, 1249, 1991.
247. **Shukri, Z. A. and Champness, C. H.**, *Surface Review and Letters*, 5, 419, 1998.
248. **Contreras, M. A., Egaas, B., King, D., Swartzlander, A., and Dullweber, T.**, *Thin Sol. Films*, 361-362, 167, 2000.
249. **Mickelsen, R. A., Devaney, W. E., Chen, W. S., Hsiao, Y. R., and Lowe, V.**, *IEEE Trans. Elec. Dev.*, ED-31, 542, 1984.

250. **Potter, R. R., Eberspacher, C., and Fabick, L. B.**, *The Conference Record of the 18th IEEE Photovoltaic Specialists Conference*, IEEE, New York, 1659, 1985.
251. **Mauch, R. H., Hedström, J., Lincot, D., Ruckh, M., Kessler, J., Klinger, R., Stolt, L., Vedel, J., and Schock, H. W.**, *The Conference Record of the 22nd IEEE Photovoltaic Specialists Conference* 2, IEEE, Piscataway, 898, 1991.
252. **Kessler, J., Ruckh, M., Hariskos, D., Rühle, U., Menner, R., and Schock, H. W.**, *The Conference Record of the 23rd IEEE Photovoltaic Specialists Conference*, IEEE, Piscataway, 447, 1993.
253. **Lincot, D., Ortega-Borges, R., Vedel, J., Ruckh, M., Kessler, J., Velthaus, K. O., Hariskos, D., and Schock, H. W.**, *Proceedings of the 11th EC Photovoltaic Solar Energy Conference*, Harwood and Chur, Eds., Kluwer, Dordrecht, 870, 1992.
254. **Kessler, J., Velthaus, K. O., Ruckh, M., Laichinger, R., Schock, H. W., Lincot, D., Ortega, R., and Vedel, J.**, *6th International Photovoltaic Science and Engineering Conference Proceedings*, Das, B. K. and Singh, S. N., Eds., Oxford & IBH Publishing Co. Pvt. Ltd., 1005, 1992.
255. **Ramanathan, K., Wiesner, H., Ashner, S., Niles, D., Bhattacharya, R. N., Keane, J., Contreras, M. A., and Noufi, R.**, *Proceedings of the 2nd World Conference on Photovoltaic Solar Energy Conversion*, EC Joint Research Centre, Brussels, 477, 1998.
256. **Wada, T., Hayashi, S., Hashimoto, Y., Nishiwaki, S., Sato, T., Negami, T., and Nishatani, M.**, *Proceedings of the 2nd World Conference on Photovoltaic Solar Energy Conversion*, EC Joint Research Centre, Brussels, 403, 1998.
257. **Kylner, A.**, *J. Electroch. Soc.*, 146, 1816, 1999.
258. **Kronik, L., Burstein, L., Leibovitch, M., Shapira, Y., Ga., D., Moons, E., Beir, J., Hodes, G., Cahen, D., Hariskos, K., Klenk, R., and Schock, H.-W.**, *Appl. Phys. Lett.*, 67, 1022, 1995.
259. **Li, S. S., Stanbery, B. J., Huang, C. H., Chang, C. H., Anderson, T. J., and Chang, Y. S.**, *The Conference Record of the 25th IEEE Photovoltaic Specialists Conference*, IEEE, Piscataway, 821, 1996.
260. **Huang, C. H., Li, S. S., Stanbery, B. J., Chang, C. H., and Anderson, T. J.**, *Conference Record of the 26th IEEE Photovoltaic Specialists Conference*, IEEE, Piscataway, 407, 1997.
261. **Huang, C. H., Li, S. S., Rieth, L., Halani, A., Fisher, M. L., Song, J., Anderson, T. J., and Holloway, P. H.**, *Conference Record of the 28th IEEE Photovoltaic Specialists Conference*, IEEE, Piscataway, 696, 2000.
262. **Tomar, M. S. and Garcia, F. J.**, *Thin Sol. Films*, 90, 419, 1982.
263. **Olsen, L. C., Aguilar, H., Addis, F. W., Lei, W., and Li, J.**, *The Conference Record of the 25th IEEE Photovoltaic Specialists Conference*, IEEE, Piscataway, 997, 1996.
264. **Ennaoui, A., Weber, M., Scheer, R., and Lewerenz, H. J.**, *Solar Energy Mat. and Sol. Cells*, 54, 277, 1998.
265. **Sterner, J., Kessler, J., Bodegård, M., and Stolt, L.**, *Proceedings of the 2nd World Conference on Photovoltaic Solar Energy Conversion*, EC Joint Research Centre, Brussels, 1145, 1998.
266. **Delahoy, A. E., Ruppert, A., and Contreras, M.**, *Thin Sol. Films*, 361-362, 140, 2000.
267. **Nouhi, A., Stirn, R. J., and Hermann, A.**, *The Conference Record of the 19th IEEE Photovoltaic Specialists Conference*, IEEE, Piscataway, 1461, 1987.
268. **Yoo, J.-B., Fahrenbruch, A. L., and Bube, R. H.**, *The Conference Record of the 20th IEEE Photovoltaic Specialists Conference*, IEEE, Piscataway, 1431, 1988.
269. **Ennaoui, A., Weber, M., Lokhande, C. D., Scheer, R., and Lewerenz, H. J.**, *Proceedings of the 2nd World Conference on Photovoltaic Solar Energy Conversion*, EC Joint Research Centre, Brussels, 628, 1998.
270. **Engelhardt, F., Bornemann, L., Köntges, M., Meyer, T., and Parisi, J.**, *Proceedings of the 2nd World Conference on Photovoltaic Solar Energy Conversion*, EC Joint Research Centre, Brussels, 1153, 1998.
271. **Konagai, M., Ohtake, Y., and Okamoto, H.**, *Thin Films for Photovoltaic and Related Device Applications*, MRS Symposium Proceedings 426, Ginley, D. et al., Eds., Materials Research Society, Pittsburgh, 153, 1996.
272. **Ohtake, Y., Ichikawa, M., Okamoto, T., Yamada, A., Konagai, M., and Saito, K.**, *The Conference Record of the 25th IEEE Photovoltaic Specialists Conference*, IEEE, Piscataway, 793, 1996.
273. **Yamada, A., Chaisitsak, S., Ohtake, Y., and Konagai, M.**, *Proceedings of the 2nd World Conference on Photovoltaic Solar Energy Conversion*, EC Joint Research Centre, Brussels, 1177, 1998.
274. **Kushiya, K., Kuriyagawa, S., Nii, T., Sugiyama, I., Kase, T., Sato, M., and Takeshita, H.**, *Proc. 13th EC Photovoltaic Solar Energy Conf.*, 2016, 1995.
275. **Kushiya, K., Nii, T., Sugiyama, I., Satoh, Y., Inamori, Y., and Takeshita, H.**, *Jpn. J. Appl. Phys.*, 35, 4383, 1996.
276. **Nakada, T. and Mizutani, M.**, *Conference Record of the 28th IEEE Photovoltaic Specialists Conference*, IEEE, Piscataway, 529, 2000.
277. **Nakada, T.**, *II–VI Compound Semiconductor Photovoltaic Materials*, MRS Symposium Proceedings 668, Birkmire, R. et al., Eds., MRS, Warrendale, H7.1.1, 2001.
278. **Velthaus, K. O., Kessler, J., Ruckh, M., Hariskos, D., Schmid, D., and Schock, H. W.**, *Proceedings of the 11th EC Photovoltaic Solar Energy Conference*, Harwood and Chur, Eds., Kluwer, Dordrecht, 842, 1992.
279. **Hariskos, D., Ruckh, M., Rühle, U., Walter, T., and Schock, H. W.**, *Proceedings of the 1st World*

Conference on Photovoltaic Energy Conversion, IEEE, Piscataway, 91, 1994.

280. **Braunger, D., Hariskos, D., Walter, T., and Schock, H. W.**, *Solar Energy Mat. and Sol. Cells*, 40, 97, 1996.
281. **Hariskos, D., Ruckh, M., Rühle, U., Walter, T., Schock, H. W., Hedström, J., and Stolt, L.**, *Solar Energy Mat. and Sol. Cells*, 41/42, 345, 1996.
282. **Bayón, R., Guillén, C., Martinez, M. A., Gutiérrez, M. T., and Herrero, J.**, *J. Electroch. Soc.*, 145, 2775, 1998.
283. **Huang, C. H., Li, S. S., Shafarman, W. N., Chang, C. H., Lambers, E. S., Rieth, L., Johnson, J. W., Kim, S., Stanbery, B. J., and Anderson, T. J.**, *Technical Digest of the 11th International Photovoltaic Science and Engineering Conference*, Tokyo University of Agric and Tech., Tokyo, 855, 1999.
284. **Bayón, R., Maffiotte, C., and Herrero, J.**, *Thin Sol. Films*, 353, 100, 1999.
285. **Kaufmann, C., Dobson, P. J., Neve, S., Bohne, W., Klaer, J., Klenk, R., Pettenkofer, C., Röhrich, J., Scheer, R., and Störkel, U.**, *Conference Record of the 28th IEEE Photovoltaic Specialists Conference*, IEEE, Piscataway, 688, 2000.
286. **Mickelsen, R. A. and Chen, W. S.**, *The Conference Record of the 16th IEEE Photovoltaic Specialists Conference*, IEEE, Piscataway, 781, 1983.
287. **Ahrenkiel, R. K., Kazmerski, L. L., Matson, R. J., Osterwald, C., Massopust, T. P., Mickelsen, R. A., and Chen, W. S.**, *Appl. Phys. Lett.*, 43, 658, 1983.
288. **Matson, R. J., Noufi, R., Ahrenkiel, R. K., Powell, R. C., and Cahen, D.**, *Solar Cells*, 16, 495, 1986.
289. **Kushiya, K., Hakuma, H., Sano, H., Yamada, A., and Konagai, M.**, *Solar Energy Mat. and Sol. Cells*, 35, 223, 1994.
290. **Dirnstorfer, I., Hofmann, D. M., Meister, D., and Meyer, B. K.**, *Proceedings of the 2nd World Conference on Photovoltaic Solar Energy Conversion*, EC Joint Research Centre, Brussels, 1165, 1998.
291. **Nakada, T.**, *Thin Sol. Films*, 361-362, 346, 2000.
292. **Birkmire, R. W., Hall, R. B., and Phillips, J. E.**, *The Conference Record of the 17th IEEE Photovoltaic Specialists Conference*, IEEE, New York, 882, 1984.
293. **Mickelsen, R. A. and Chen, W. S.**, *Appl. Phys. Lett.*, 36, 371, 1980.
294. **Kapur, V., Singh, P., Choudary, U. V., Uno, F. M., Elyash, L., and Meisel, S.**, *The Conference Record of the 17th IEEE Photovoltaic Specialists Conference*, IEEE, New York, 777, 1984.
295. **Wada, T.**, *Solar Energy Mat. Sol. Cells*, 49, 249, 1997.
296. **Schmid, D., Ruckh, M., and Schock, H. W.**, *Proceedings of the 1st World Conference on Photovoltaic Energy Conversion* 1, IEEE, Piscataway, 198, 1994.
297. **Ermer, J., Gay, R., Pier, D., and Tarrant, D.**, *J. Vac. Sci. Tech. A*, 11, 1888, 1993.
298. **Yang, L. C. and Rockett, A.**, *J. Appl. Phys.*, 75, 1185, 1994.
299. **Roy, M. and Philips, J. M.**, *The Conference Record of the 20th IEEE Photovoltaic Specialists Conference*, IEEE, Piscataway, 1618, 1988.
300. **Lee, Y.-J. and Gray, J. L.**, *The 1st World Conference on Photovoltaic Energy Conversion*, IEEE, Piscataway, 287, 1994.
301. **Roy, M. and Philips, J. M.**, *The Conference Record of the 21st IEEE Photovoltaic Specialists Conference*, IEEE, Piscataway, 743, 1990.
302. **Shafarman, W. N. and Phillips, J. E.**, *The Conference Record of the 22nd IEEE Photovoltaic Specialists Conference*, IEEE, New York, 934, 1991.
303. **Böer, K. W. and Hall, R. B.**, *J. Appl. Phys.*, 37, 4739, 1966.
304. **Stanbery, B. J., Chen, W. S., and Mickelsen, R. A.**, *Materials and New Processing Technologies for Photovoltaics*, The Electrochemical Society Symposium PV 85-9, Kapur, V. K., Dismukes, J. P., and Pizzini, S., Eds., The Electrochemical Society, Pittsburgh, 115, 1984.
305. **Mitchell, K. W., Eberspacher, C., Ermer, J., and Pier, D.**, *The Conference Record of the 20th IEEE Photovoltaic Specialists Conference*, IEEE, Piscataway, 1384, 1988.
306. **Birkmire, R. W., Shafarman, W. N., and Varrin, R. D., Jr.**, *Conference Record of the 21st IEEE Photovoltaic Specialists Conference* 1, IEEE, New York, 550, 1990.
307. **Nakada, T. and Mise, T.**, *17th European Photovoltaic Solar Energy Conference and Exhibition*, Munich, 2001, in press.
308. **Nakada, T., Okano, N., Tanaka, Y., Fukuda, H., and Kunioka, A.**, *The Conference Record of the 25th IEEE Photovoltaic Specialists Conference*, IEEE, Piscataway, 95, 1994.
309. **Negami, T., Nishitani, M., Ikeda, M., and Wada, T.**, *Solar Energy Mat. and Sol. Cells*, 35, 215, 1995.
310. **Nakada, T., Kume, T., and Kunioka, A.**, *The Conference Record of the 25th IEEE Photovoltaic Specialists Conference*, IEEE, Piscataway, 893, 1996.
311. **Bhattacharya, R. N.**, *J. Electroch. Soc.*, 130, 2040, 1983.
312. **Guillemoles, J.-F., Cowache, P., Lusson, A., Fezzaa, K., Boisivon, F., Vedel, J., and Lincot, D.**, *J. Appl. Phys.*, 79, 7293, 1996.
313. **Thornton, J. A. and Lommasson, T. C.**, *Solar Cells*, 16, 165, 1986.
314. **Lommasson, T. C., Talieh, H., Meakin, J. D., and Thornton, J. A.**, *The Conference Record of the 19th IEEE Photovoltaic Specialists Conference*, IEEE, New York, 1285, 1987.
315. **Elliott, E., Tomlinson, R. D., Parkes, J., and Hampshire, M. J.**, *Thin Sol. Films*, 20, S25, 1974.
316. **Arya, R. R., Russel, T. C., Narashimham, M. C., Case, C. J., Beaulieu, R., and Loferski, J. J.**, *The Conference Record of the 17th IEEE Photovoltaic Specialists Conference*, IEEE, New York, 764, 1984.

317. **Sagnes, B., Salesse, A., Artaud, M. C., Duchemin, S., Bougnot, J., and Bougnot, G.**, *J. Crystal Growth*, 124, 620, 1992.
318. **Talieh, H. and Rockett, A.**, *Solar Cells*, 27, 321, 1989.
319. **Thornton, J. A., Cornog, D. G., Hall, R. B., Shea, S. P., and Meakin, J. D.**, *J. Vac. Sci. Tech. A*, 2, 307, 1984.
320. **Rockett, A., Lommasson, T. C., Campos, P., Yang, L. C., and Talieh, H.**, *Thin Sol. Films*, 171, 109, 1989.
321. **Shafarman, W. N. and Zhu, J.**, *II–VI Compound Semiconductor Photovoltaic Materials*, MRS Symposium Proceedings 668, Birkmire, R. et al., Eds., MRS, Warrendale, H2.3.1, 2001.
322. **Don, E. R., Hill, R., and Russell, G. J.**, *Solar Cells*, 16, 131, 1986.
323. **Stanbery, B. J., Chen, W. S., Devaney, W. E., and Stewart, J. M.**, Phase 1 Annual Subcontract Report NREL contract ZH-1-19019-6, 1992.
324. **Klenk, R., Walter, T., Schimd, D., and Schock, H. W.**, *Jap. J. Appl. Phys.*, 32 Supplement 32–3, 57, 1993.
325. **Tuttle, J. R., Contreras, M., Tennant, A., Albin, D., and Noufi, R.**, *The Conference Record of the 23rd IEEE Photovoltaic Specialists Conference* 1, IEEE, Piscataway, 415, 1993.
326. **Bode, M. H., Al-Jassim, M. M., Jones, K. M., Ratson, R., and Hasoon, F.**, *Photovoltaic Advanced Research and Development Review Meeting*, AIP Conference Proceedings 268, Noufi, R., Eds., AIP, Woodbury, 140, 1992.
327. **Tuttle, J. R., Contreras, M., Bode, M. H., Niles, D., Albin, D. S., Matson, R., Gabor, A. M., Tennant, A., Duda, A., and Noufi, R.**, *J. Appl. Phys.*, 77, 153, 1995.
328. **Gabor, A. M., Tuttle, J. R., Albin, D. S., Contreras, M. A., Noufi, R., and Hermann, A. M.**, *Appl. Phys. Lett.*, 65, 198, 1994.
329. **Gabor, A. M., Tuttle, J. R., Contreras, M., Albin, D. S., Franz, A., Niles, D. W., and Noufi, R.**, *Proceedings of the 12th European Photovoltaic Solar Energy Conference*, Amsterdam, 939, 1994.
330. **AbuShama, J., Noufi, R., Yan, Y., Jones, K., Keys, B., Dippo, P., Romero, M., Al-Jassim, M. M., Alleman, J., and Williamson, D. L.**, *II–VI Compound Semiconductor Photovoltaic Materials*, MRS Symposium Proceedings 668, Birkmire, R. et al., Eds., MRS, Warrendale, H7.2.1, 2001.
331. **Binsma, J. J. M. and van der Linden, H. A.**, *Thin Sol. Films*, 97, 237, 1982.
332. **Chu, T. L., Chu, S. S., Lin, S. C., and Yue, J.**, *J. Electroch. Soc.*, 131, 2182, 1984.
333. **Kapur, V., Basol, B., and Tseng, E. S.**, *The Conference Record of the 18th IEEE Photovoltaic Specialists Conference*, IEEE, New York, 1429, 1985.
334. **Basol, B. and Kapur, V.**, *Appl. Phys. Lett.*, 54, 1918, 1989.
335. **Marudachalam, M., Birkmire, R., Schultz, J. M., and Yokimcus, T.**, *The Conference Record of the 25th IEEE Photovoltaic Specialists Conference*, IEEE, Piscataway, 234, 1996.
336. **Basol, B.**, *J. Vac. Sci. Tech. A*, 10, 2006, 1992.
337. **Knowles, A., Oumous, H., Carter, M. J., and Hill, R.**, *The Conference Record of the 20th IEEE Photovoltaic Specialists Conference* 2, IEEE, New York, 1482, 1988.
338. **Knowles, A., Oumous, H., Carter, M. J., and Hill, R.**, *Semicond. Sci. Technol.*, 3, 1143, 1988.
339. **Karg, F., Probst, V., Harms, H., Rimmasch, J., Riedl, W., Kotschy, J., Holz, J., Treichler, R., Eibl, O., Mitwalsky, A., and Kiendl, A.**, *The Conference Record of the 23rd IEEE Photovoltaic Specialists Conference*, IEEE, Piscataway, 441, 1993.
340. **Matsushita, H. and Takizawa, T.**, *Jpn. J. Appl. Phys.*, 34, 4699, 1995.
341. **Wolf, D. and Muller, G.**, *Thin Sol. Films*, 361-362, 155, 2000.
342. **Nakada, T., Ichien, T., Ochi, T., and Kunioka, A.**, *Proceedings of the 11th EC Photovoltaic Solar Energy Conference*, Harwood and Chur, Eds., Kluwer, Dordrecht, 794, 1992.
343. **Chang, C.-H., Stanbery, B. J., Morrone, A. A., Davydov, A., and Anderson, T. J.**, *Thin-Film Structures for Photovoltaics*, MRS Symposium Proceedings 485, Jones, E. D., et al., Eds., MRS, Warrendale, 163, 1997.
344. **Beck, M. E., Swartzlander-Guest, A., Matson, R., Keane, J., and Noufi, R.**, *Solar Energy Mat. and Sol. Cells*, 64, 135, 2000.
345. **Wolf, D. and Müller, G.**, *Thin-Film Structures for Photovoltaics*, MRS Symposium Proceedings 485, Jones, E. D., et al., Eds., MRS, Warrendale, 173, 1997.
346. **Arita, T., Suyama, N., Kita, Y., Kitamura, S., Hibino, T., Takada, H., Omura, K., Ueno, N., and Murozono, M.**, *The Conference Record of the 20th IEEE Photovoltaic Specialists Conference*, IEEE, New York, 1650, 1988.
347. **Eberspacher, C., Pauls, K., and Serra, J.**, *Conference Record of the 28th IEEE Photovoltaic Specialists Conference*, IEEE, Piscataway, 517, 2000.
348. **Kapur, V., Fisher, M. L., and Roe, R.**, *II–VI Compound Semiconductor Photovoltaic Materials*, MRS Symposium Proceedings 668, Birkmire, R., et al., Eds., MRS, Warrendale, H2.6.1, 2001.
349. **Liu, X. X. and Sites, J. R.**, *J. Appl. Phys.*, 75, 577, 1994.
350. **Potter, R. R. and Sites, J. R.**, *The Conference Record of the 16th IEEE Photovoltaic Specialists Conference*, IEEE, New York, 475, 1982.
351. **Ruberto, M. N. and Rothwarf, A.**, *J. Appl. Phys.*, 61, 4662, 1987.
352. **Miller, W. A. and Olsen, L. C.**, *IEEE Trans. Elec. Dev.*, ED-31, 654, 1984.

353. **Burgelman, M., Nollet, P., Degrave, S., and Beier, J.**, *Conference Record of the 28th IEEE Photovoltaic Specialists Conference*, IEEE, Piscataway, 551, 2000.
354. **McMahon, T. J. and Fahrenbruch, A. L.**, *Conference Record of the 28th IEEE Photovoltaic Specialists Conference*, IEEE, Piscataway, 539, 2000.
355. **Niemeegers, A., Burgelman, M., Herberholz, R., Rau, U., Hariskos, D., and Schock, H. W.**, *Prog. Photovolt: Res. Appl.*, 6, 407, 1998.
356. **Shafarman, W. N. and Phillips, J. E.**, *The Conference Record of the 23rd IEEE Photovoltaic Specialists Conference*, IEEE, Piscataway, 453, 1993.
357. **Hou, J., Fonash, S. J., and Kessler, J.**, *The Conference Record of the 25th IEEE Photovoltaic Specialists Conference*, IEEE, Piscataway, 961, 1996.
358. **Topic, M., Smole, F., and Furlan, J.**, *Solar Energy Mat. and Sol. Cells*, 49, 311, 1997.
359. **Feucht, D. L.**, *J. Vacuum Sci. Technol.*, 14, 57, 1977.
360. **Rothwarf, A.**, *The Conference Record of the 16th IEEE Photovoltaic Specialists Conference*, IEEE, New York, 791, 1982.
361. **Matson, R. J., Herrington, C. R., Noufi, R., and Powell, R. C.**, *The Conference Record of the 18th IEEE Photovoltaic Specialists Conference*, IEEE, New York, 1648, 1985.
362. **Matson, R. J., Noufi, R., Backmann, K. J., and Cahen, D.**, *Ternary and Multinary Compounds, Proceedings of the 7th International Conference*, Deb, S. K. and Zunger, A., Eds., Materials Research Society, Pittsburgh, 65, 1986.
363. **Rau, U., Jasenek, A., Herberholz, R., Schock, H.-W., Guillemoles, J.-F., Lincot, D., and Kronik, L.**, *Proceedings of the 2nd World Conference on Photovoltaic Solar Energy Conversion*, EC Joint Research Centre, Brussels, 428, 1998.
364. **Ramanathan, K., Hasoon, F., Smith, S., Mascarenhas, A., Al-Thani, H., Alleman, J., Ullal, H. S., and Keane, J.**, *Conference Record of the 29th IEEE Photovoltaic Specialists Conference*, IEEE, Piscataway, in press, 2002.
365. **Ali, A. Y. and Böer, K. W.**, *The Conference Record of the 18th IEEE Photovoltaic Specialists Conference*, IEEE, Piscataway, 1739, 1985.
366. **Schwartz, R. J., Gray, J. L., and Lee, Y. J.**, *The Conference Record of the 22nd IEEE Photovoltaic Specialists Conference* 2, IEEE, New York, 920, 1991.
367. **Sasala, R. A. and Sites, J. R.**, *The Conference Record of the 23rd IEEE Photovoltaic Specialists Conference*, IEEE, Piscataway, 543, 1993.
368. **Willett, D. and Kuriyagawa, S.**, *The Conference Record of the 23rd IEEE Photovoltaic Specialists Conference*, IEEE, Piscataway, 495, 1993.
369. **Cahen, D. and Chernyak, L.**, *Adv. Mater.*, 9, 861, 1997.
370. **Igalson, M. and Schock, H. W.**, *J. Appl. Phys.*, 80, 5765, 1996.
371. **Meyer, T., Engelhardt, F., Parisi, J., Riedl, W., Karg, F., Schmidt, M., and Rau, U.**, *Proceedings of the 2nd World Conference on Photovoltaic Solar Energy Conversion*, EC Joint Research Centre, Brussels, 1157, 1998.
372. **Rau, U., Weinert, K., Nguyen, Q., Mamor, M., Hanna, G., Jasenek, A., and Schock, H. W.**, *II–VI Compound Semiconductor Photovoltaic Materials*, MRS Symposium Proceedings 668, Birkmire, R., et al., Eds., MRS, Warrendale, H9.1.1, 2001.
373. **Guilinger, J.**, NREL RAF-9-29609, 1999.
374. **Zweibel, K.** (personal communication), 2001.

Copyright © 2002 EBSCO Publishing